UNIVERSITY OF THESSALY

SCHOOL OF ENGINEERING

DEPARTMENT OF MECHANICAL ENGINEERING

MODELLING THE DYNAMIC BEHAVIOR OF THE PULMONARY SURFACTANT

by

GERASIMOS KARATSALOS

Submitted in partial fulfillment of the requirements for the degree of Master of Science in Mechanical Engineering at the University of Thessaly

Volos, 2024

Approved by the Committee on Final Examination:

Advisor	Dr. Vasilis Bontozoglou, Professor, Department of Mechanical Engineering, University of Thessaly
Member	Dr. Nikolaos Pelekasis, Professor, Department of Mechanical Engineering, University of Thessaly
Member	Dr. Georgios Charalampous, Assistant Professor, Department of Mechanical Engineering, University of Thessaly

Date Approved: [March 07, 2024]

MODELLING THE DYNAMIC BEHAVIOR OF THE PULMONARY SURFACTANT

GERASIMOS KARATSALOS

Department of Mechanical Engineering, University of Thessaly

Supervisor: Dr Vasilis Bontozoglou

Professor

Abstract

The pulmonary surfactant plays a crucial role in the function of the human respiratory system and its structure and behavior has been thoroughly investigated through the years. In this thesis the pulmonary surfactant and its components, as well as important properties of interfaces are analyzed. In addition, the equilibrium and dynamic behavior of surfactants and important phenomena such as the collapse phenomenon are also examined. Lastly, by using a recently developped model by Bouchoris and Bontozoglou (A model of lung surfactant dynamics based on intrinsic interfacial compressibility), the effect of various parameters on the model under dynamic conditions are examined.

Table of contents

LIST OF TABLES

LIST OF FIGURES

Chapter 1. **INTRODUCTION**

1.1 Motivation

The pulmonary surfactant is vital for the human organism. It is a complex system of lipids and proteins. In addition, synthetic pulmonary are being developed and pulmonary surfactant is being extracted from animals to use as replacement [1]. The consistency of those solutions can vary. To predict the behavior of surfactant under different conditions and different consistencies various models have been developed which vary in complexity. This thesis aims to understand how parameters change the behavior of surfactants under dynamic conditions.

1.2 Diploma Thesis Organization

The rest of this thesis is divided into four parts which include chapters 2-6. Specifically:

In Chapter 2 the basic components and concepts surrounding the pulmonary surfactants are discussed. This includes the structure of the surfactants, the consistency of the pulmonary surfactant, surface tension, surface pressure and surface excess.

In Chapter 3 the surface of a solution that has surfactant under equilibrium is examined which follows the introduction of important isotherms. The behavior of the surfactant under dynamic conditions is also introduced. Lastly, important phenomena and concepts are examined which include the Marangoni effects, the elasticity, the compressibility, the micelle formation and the collapse phenomenon.

In Chapter 4 the model developped by Bouchoris and Bontozoglou [21] is presented.

In Chapter 5 the results of the various changes in paramerers are shown.

In Chapter 6 the results are discussed.

Chapter 2. **LITERATURE REVIEW**

2.1 Structure of the respiratory system

The main function of the human respiratory system is to provide enough surface area for the gas exchange between O2 and CO2 while proving protection against outside threats [2]. It consists of three major compartments: the extrathoracic region, extending from the nose or the mouth to the entrance of the trachea, the tracheobronchial region, ranging from the trachea to the terminal bronchioles, and the acinar or alveolar-interstitial or pulmonary region, where gas exchange takes place between air and blood via the alveoli [1], (ICRP 1994). The size of a single alveolus ranges from $3.3\ to\ 4.8x10^6 \mu m^3$. In total the alveoli are numbered to be around $3x10^8$ that provide an area of about $90m^2$ for gas exchange [4]. At normal conditions, the human breathing frequency is 0.04–0.2 Hz [5].

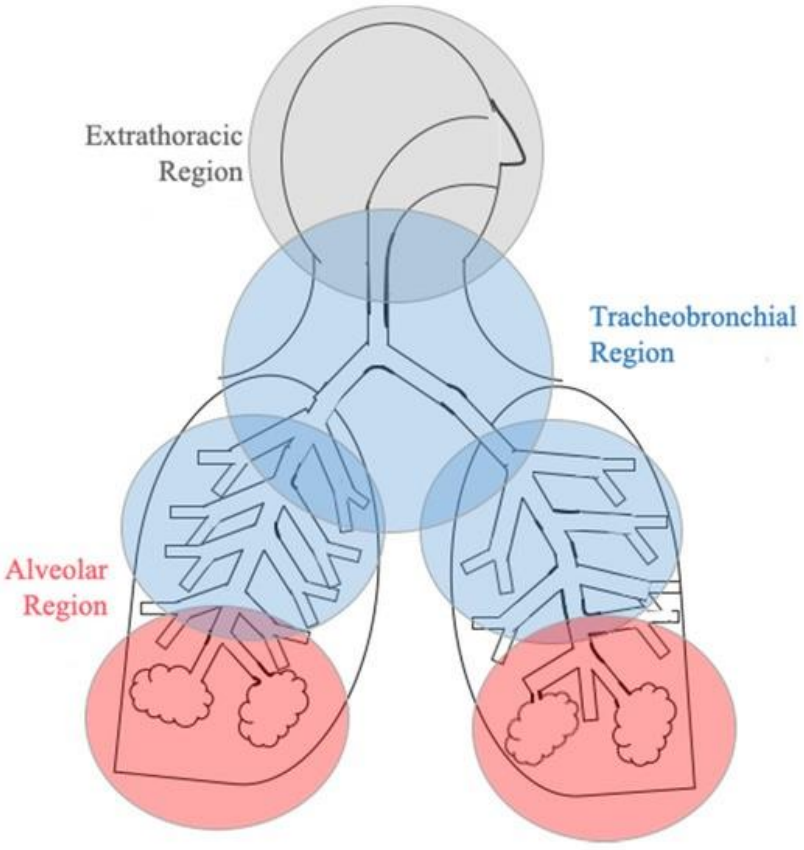

Figure 2.1: The three major parts of the human respiratory system. The extrathoracic region colored in grey, the tracheobronchial region colored in blue, and the alveolar region colored in red (Sagona et al.).

2.2 The importance of surface tension

In cases where the human body does not produce adequate amounts of pulmonary surfactant for example at prematurely born infants, the stiffness of the lungs due to high surface tension does not allow normal breathing to take place and ventilation is rendered difficult. With the application of surfactant replacement therapy these problems can be confronted [6].

While exhaling, the alveoli reduce their surface area. This in turn, according to the Laplace law [7] eq. (1.1) will increase the pressure inside the alveoli. The alveoli are not isolated but are interconnected. The inevitable pressure difference between the alveoli that are at proximity will result in the over inflation of one alveolus and the collapse of the rest. The pulmonary surfactant will prevent this phenomenon from occurring by counteracting the pressure difference with the change of the surface tension. The over inflation of one alveolus will decrease the effect of the pulmonary surfactant (increasing the surface tension), while the compression of other alveoli will increase the effect of the pulmonary surfactant (decreasing the surface tension). The mechanisms by which the effectiveness of the pulmonary surfactant change will be discussed below.

$$\mathrm{P} = 2\frac{\sigma}{\mathrm{r}} \tag{1.1}$$

Where P is the pressure in a sphere, σ is the surface tension and r is the radius of a sphere.

2.3 Surfactants

Most surfactants are amphiphilic molecules that consist of a hydrophobic tail and a hydrophilic head group [7], [8]. The dissolved form, although it increases the entropy of the system, is not as energetically efficient as the precipitated form that minimize energetically unfavorable interactions [8]. Depending on the concentration of the surfactants in the bulk of the fluid, they are described as soluble or insoluble. When the concentration in the bulk is immeasurably small the surfactant is insoluble. Gibbs monolayers are formed by soluble surfactants and they portray the balance between the dissolved molecules and the ones adsorbed to the surface. Monolayers formed by insoluble surfactants are called Langmuir monolayers. Insoluble surfactants do not change the number of surfactants in the monolayer when changes on the surface take place [8].

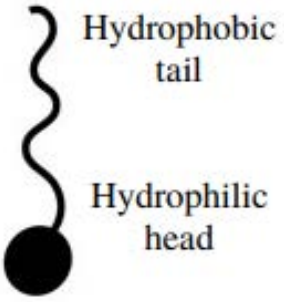

Figure 2.2: Schematic representation of an amphiphilic molecule [5].

2.4 The pulmonary surfactant system

The alveoli are coated in a thin protected layer, the pulmonary surfactant which plays a functional and protective role in the operation of the respiratory system. It greatly reduces the surface tension of the alveoli, very close to 0 mN/m, decreases the tendency for alveolar collapse [9] and protects the human body from outside threats that exist in the air. It consists of a mixture of lipids (90%), the most dominant of which being dipalmitoylphosphatidylcholine (DPPC) and the proteins (10%) SP-A, SP-B, SP-C and SP-D [10]. The reduction of the surface tension is mainly the role of the lipids, but they are unable to adsorb quickly enough in the constantly inflating and deflating alveoli [9]. The proteins SP-B and SP-C are hydrophobic and therefore surface active allow the pulmonary surfactant film to reach high pressures but also retain substantial flexibility which is vital for respreading during expansion [11]. SP-B is also vital for the process of adsorption. In addition, SP-A and SP-D, are a significant protective factor of innate immunity [12]. SP-A also works in favor of lipid adsorption and film formation but only in the presence of SP-B [13]. Depending on the surface pressure the pulmonary surfactant changes its distribution across the surface and depending on the way the surfactant molecules are arranged, their phase varies fig. 2.4. At large areas per molecule, surfactants are in the gaseous state where the hydrophobic portions of the molecule make significant contact with the water surface, but little contact with each other [1]. At very low values of surface coverage, the surfactant molecules are in a liquid expanded (LE) phase where the effect of the surfactants is negligible for the act of lowering surface tension. As the surface pressure rises, the liquid condense phase coexists with the (LE) phase until the (LC) becomes dominant. The (LC) phase is characterized by high surface pressure, low moral area Ω and a high angle of the tails of the surfactants (close to being vertical). The over-compression of the pulmonary surfactant will cause the collapse of the monolayer created

by the surfactants which creates 3d_structures. The collapse mechanism is a critical factor that affects the speed of the reformation after the occurrence of the collapse [14].

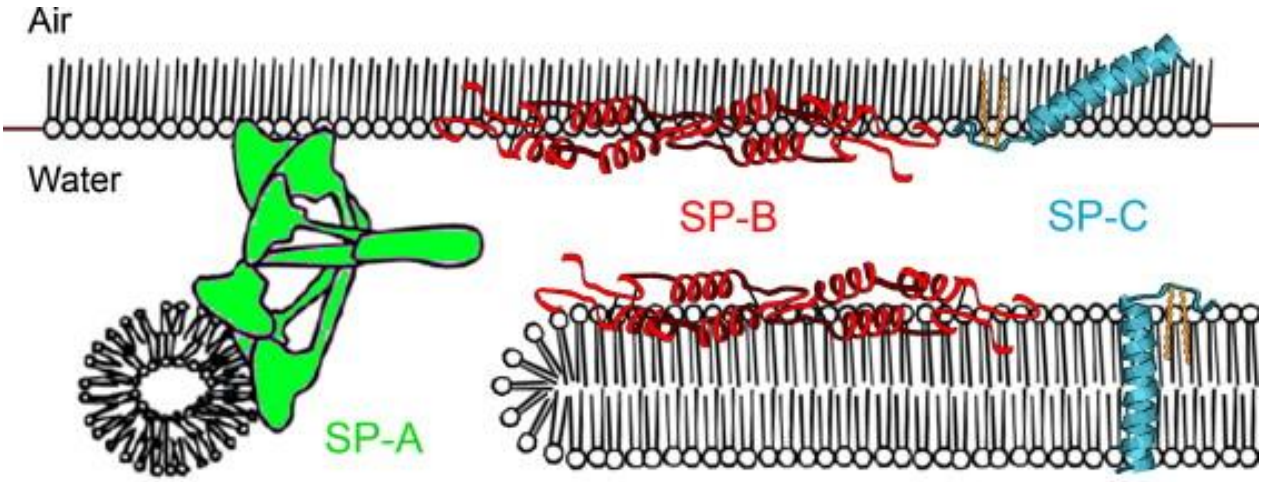

Figure 2.3: Pulmonary surfactant monolayer along with its proteins (Parra and Pérez-Gil).

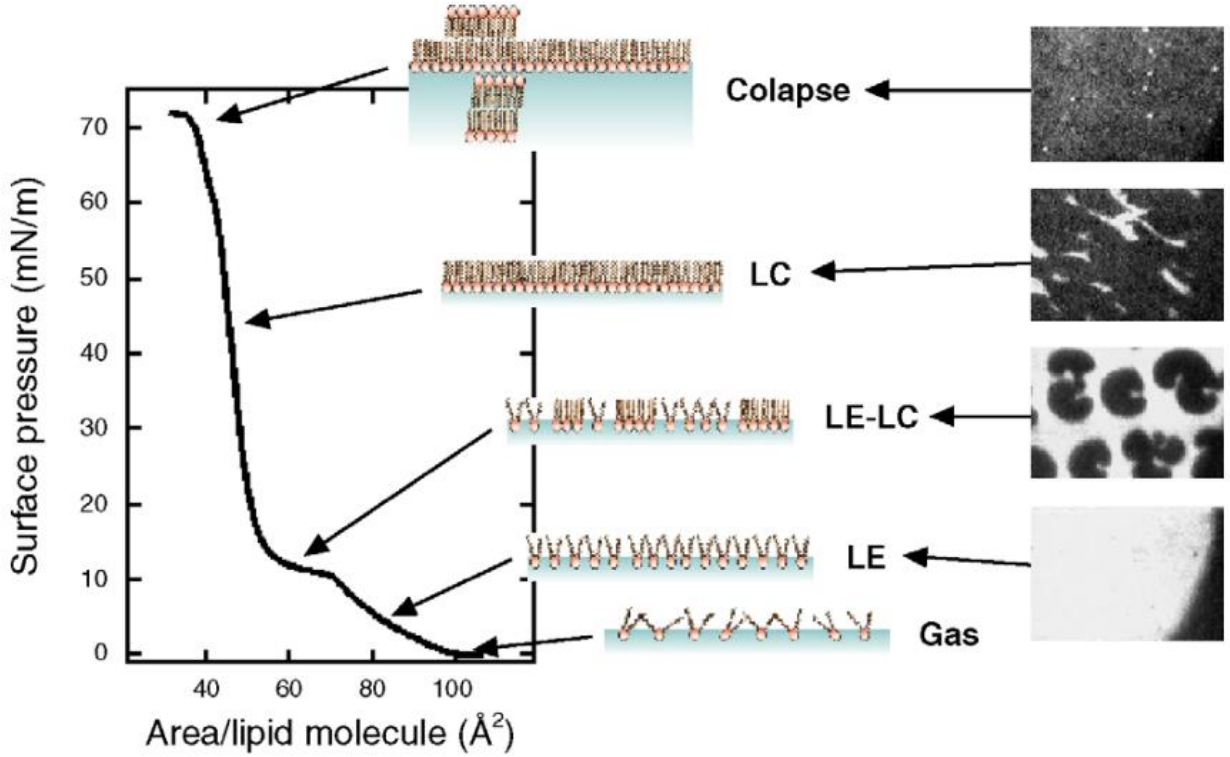

Figure 2.4: A typical Π – A (surface pressure - area/molecule) curve at specific temperature. Every segment of the curves represents a different phase state at which the adsorbed molecules are [10].

2.5 Surface tension

At the condensed phase, molecules are attracted by each other by intermolecular forces such as van der Waals forces. In the bulk the effects of the intermolecular forces are being neutralized by the existence of the surrounding molecules. Molecules near the surface on the other hand, are partly surrounded by them which is energetically unfavorable. The surface tension σ (j/m^2) of a fluid-fluid interface is associated with the energy needed to create excess area [8]. More specifically surface tension is the proportional constant that correlates the work dW needed to increase the surface area of an interface dA eq.2.1. For reference the air to water surface tension is around 0.072 j/m^2 at 25°C [7],[8].

$$\mathrm{dW} = \sigma \mathrm{dA} \qquad (2.1)$$

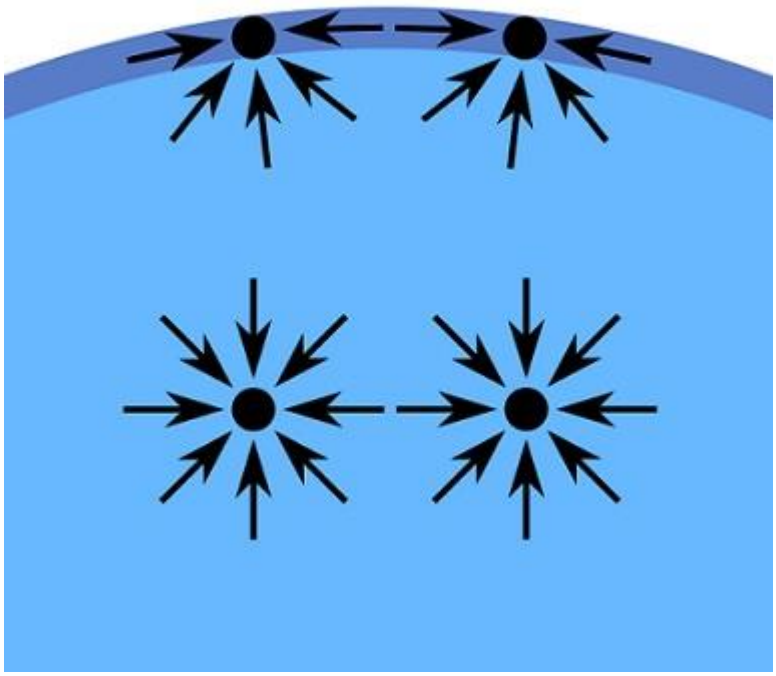

Figure 2.5: Surface tension as the result of the intermolecular forces on an interface (Nipun).

2.6 Surface pressure

Surface pressure Π (N/m) is the difference between the surface tension σ_0 of a clean subphase and that of a subphase with a monolayer σ [15].

$$\Pi = \sigma_0 - \sigma \qquad (2.2)$$

Where the term σ_0 represents the surface tension of the air to water interface in the absence of surfactants at the physiological temperature of 37 °C. σ_0 is calculated to be about 70 mN m^{-1} [16], [8].

2.7 Surface excess

When two phases are in contact, there is no clear boundary that indicates the end of the liquid phase and the start of the vapor phase but there is the interfacial region where its properties continuously and swiftly change [17]. For simplification there are two main models. The Gibbs convention where the interfacial region is replaced by a boundary layer of zero volume and surface area A and the Guggenheim's model which replaces the interfacial region with a finite surface volume [7], [8].

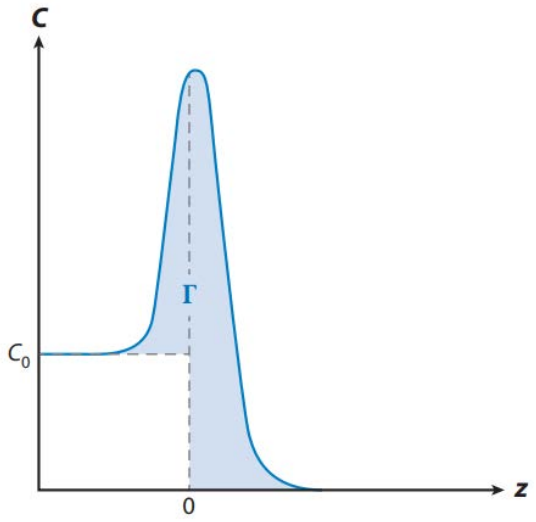

Figure 2.6: Concentration versus the position of a system with two phases [8].

At equilibrium using the Gibbs convention the interface is reduced to an infinitely thin boundary layer [7],[8]. Properties such as concentration of the interface are expressed through the boundary layer or dividing plane. Using the Gibbs convention, surface concentration or interfacial excess Γ is defined as the number of molecules or mols that exist on the boundary layer [7].

$$\Gamma = \frac{N}{A} \qquad (2.3)$$

Where N the number of molecules or molls and A the interfacial area.

Chapter 3. **THERMODYNAMICS OF SURFACES**

3.1 Equilibrium surface behavior

Under equilibrium there is balance between the adsorbed surfactants and the surfactants residing in the bulk. This equilibrium comes from the favorable enthalpy change and the unfavorable entropy decrease when the process of adsorption takes place [8]. In this case there are two phases a, b and the interface s. The Helmholtz Free Energy F is used to describe thermodynamically the system.

$$\mathrm{F} = \mathrm{U} - \mathrm{TS} \qquad (3.1)$$

Where U is the internal energy, T is the temperature and S is the entropy. For a system the internal energy is as follows.

$$\mathrm{dU} = \mathrm{TdS} - \mathrm{PdV} + \sum_{\mathrm{i}=1}^{\mathrm{N}} (\mu_{\mathrm{i}} \mathrm{dn_i}) + \mathrm{dW} \qquad (3.2)$$

Where P is the pressure, V is the volume, μ_i is the chemical potential of the i^{th} substance, n_i is the number of molecules of the i^{th} substance and W is the work done on the system without the expansion work PdV which in this case will be the surface work σdA [7] where σ is the surface tension A is the surface area. Assuming equilibrium, the chemical potential of each substance will be equal in all phases and using the Gibbs convention the interface of the system has no volume ($V^s = 0$).

$$\mu_{\mathrm{i}}{}^{\mathrm{a}} = \mu_{\mathrm{i}}{}^{\mathrm{b}} = \mu_{\mathrm{i}}{}^{\mathrm{s}} = \mu_{\mathrm{i}} \qquad (3.3)$$

For the interface an infinitely small and reversible change in the Helmholtz energy is described as:

$$\mathrm{dF^s} = -\mathrm{S^s dT} + \sum_{\mathrm{i}=1}^{\mathrm{N}} (\mu_{\mathrm{i}}{}^{\mathrm{s}} \mathrm{dn_i^s}) + \sigma \mathrm{dA} \qquad (3.4)$$

Keeping the area, the temperature and the amount of material constant leads to:

$$\mathrm{F^s} = -\mathrm{S^s T} + \sum_{\mathrm{i}=1}^{\mathrm{N}} (\mu_{\mathrm{i}}{}^{\mathrm{s}} \mathrm{dn_i^s}) + \sigma \mathrm{A} \qquad (3.5)$$

The differentiation of eq. (3.5):

$$dF^s = -S^s dT - TdS^s + +\sigma dA + Ad\sigma + \sum_{i=1}^{N}(\mu_i dn_i{}^s) + \sum_{i=1}^{N}(d\mu_i n_i{}^s) \quad (3.6)$$

Equating eq. (3.4, 3.6) gives the Guggenheim equation:

$$s^s dT + \sum_{i=1}^{N}(\Gamma_i d\mu_i) + d\sigma = 0 \quad (3.7)$$

Where s^s is the entropy per unit of surface area and $\Gamma_i = \frac{n_i{}^s}{A}$ is the surface excess which was previously mentioned. By adjusting the location of the surface of a system that consists of two components 1,2 with surface excesses of Γ_1 and Γ_2 respectively so that $\Gamma_1 = 0$ the Guggenheim equation can be written as follows:

$$d\sigma = -\Gamma_2 d\mu_2 \quad (3.8)$$

In the general form for N surface-active agents (3.8) is written as:

$$\Gamma_i = -\frac{d\sigma}{d\mu_i} \quad (3.9)$$

The thermodynamic definition of the chemical potential paired with the Gibbs-Duhem equation:

$$d\mu_i = RTdlnC_i \quad (3.10)$$

Where R is the gas constant, T is the temperature and C_i the concentration of the i^{th} substance. The combination of (3.9) and (3.10) assuming a single species of surface-active agents so that N=1 and $\Gamma_i = \Gamma$ gives the Gibbs isotherm.

$$\Gamma(C) = -\frac{1}{RT}\frac{d\sigma}{dlnC} \quad (3.11)$$

3.2 Isotherms

An estimation for the surface concentration can be obtained through isotherms that corelate the surface concentration Γ with the concentration C of the surfactant in the bulk at steady temperature and assuming equilibrium. Using isotherms, Γ is called equilibrium surface concentration. Since adsorption is a dynamic process, isotherms are also formed by assuming dynamic equilibrium where the rate of adsorption jad to the surface is equated to the rate of desorption jdes to the sub-surface [18].

$$\frac{d\Gamma}{dt} = jad - jdes = 0 \tag{3.12}$$

The Henry isotherm

The Henry isotherm corresponds to low surface concentrations Γ (gaseous state) since the interactions between the monomers on the surface are not considered. At these conditions, the adsorption flux is related to the bulk concentration and the desorption flux is related to the surface concentration Γ [8], [18].

$$ja = k_a C \tag{3.13}$$

$$jd = k_d \Gamma(C) \tag{3.14}$$

$$\Gamma(C) = \frac{k_a}{kd} C = k_h C \tag{3.15}$$

The surface equation of state for the henry isotherm is produced by combining equations (3.15) and the Gibbs equation (3.16). The equation of state correlates the interfacial tension with the adsorption [17].

$$d\sigma_{eq} = -d\Pi_{eq} = -RT\Gamma_{eq}\frac{dC}{C} \tag{3.16}$$

$$\Pi = \sigma_0 - \sigma = nRTk_h C = nRT\Gamma \tag{3.17}$$

Where n=1 for neutral molecules and n=2 for ionic molecules, Π is the surface pressure, R is the gas constant and T is the temperature.

The Langmuir isotherm

The Langmuir isotherm is based on the lattice theory. There are no interactions between the adsorbed monomers and intermolecular forces between them are omitted. The lattice is divided into sites which have equal probability to adsorb a monomer regardless of their position and the state of other sites and monomers can be adsorbed only to unoccupied sites.

The adsorption flux is adapted to consider both the number of unoccupied sites available and the concentration of surfactant in solution [7], [18].

$$ja = k_a C(\Gamma_\infty - \Gamma) \tag{3.18}$$

$$jd = k_d \Gamma \tag{3.19}$$

$$\Gamma(C) = \Gamma_\infty \frac{k_L C}{1 + k_L C} \tag{3.20}$$

Where $k_L = \frac{k_a}{kd}$. The surface equation of state for the Langmuir isotherm:

$$\Pi = nRT\Gamma_\infty \ln(1 + k_L C) \tag{3.21}$$

The Frumkin isotherm

The Frumkin isotherm is similar to the Langmuir isotherm but in addition, also accounts for the interactions between the adsorbed monomers and the monomers in the bulk [18]. The Frumkin isotherm is most suited for non-ionic surfactants.

$$C = \frac{1}{k_f} \frac{\Gamma}{\Gamma_\infty - \Gamma} \exp\left(-2a \left(\frac{\Gamma}{\Gamma_\infty}\right)\right) \tag{3.22}$$

Where k_f is the Frumkin equilibrium adsorption constant, α represents the non-ideality of the layer. When a=0 the Frumkin isotherm is reduced to the Langmuir isotherm. The surface equation of state for the Frumkin isotherm [18]:

$$\Pi = -nRT\Gamma_\infty \ln\left(1 - \left(\frac{\Gamma}{\Gamma_\infty}\right)\right) - nRTa\Gamma_\infty \left(\frac{\Gamma}{\Gamma_\infty}\right)^2 \tag{3.23}$$

3.3 Dynamic surface tension

The surface behavior as well as the flow in bulk of the fluid at which an interface is formed, make the use of isotherms unsuitable for the calculation of the surface concentration and surface tension. Thus, the use of dynamic surface tension (DST) is applied. The flux of the monomers between the bulk of the fluid and the interface is modelled mainly through diffusion or kinetically limited models. Diffusion limited models take place when the rate at which the subsurface of the fluid and the surface are reaching equilibrium is significantly faster than the rate of the subsurface and the bulk. It is assumed that the monomers are absorbed at the surface as soon as they reach the subsurface. Kinetically limited models are applicable when the act of adsorption of the monomers from the subsurface to the interface is significantly slower than the process of diffusion from the bulk [8,18]. At the model studied in this thesis the exchange of

surfactant between the bulk and the bulk is kinetically limited. The energy barrier opposed from the adsorption of the monomers to the surface is expressed through the fluxes of adsorption (jad) and desorption (jdes) (Warszynski et al 1998), [8]:

$$\frac{1}{\mathrm{A}}\frac{\mathrm{d}(\mathrm{A}\Gamma)}{\mathrm{dt}} = \mathrm{jad}(\Gamma, \mathrm{Cs}) - \mathrm{jdes}(\Gamma) \tag{3.24}$$

$$\mathrm{jad}(\Gamma, \mathrm{Cs}) = \mathrm{kaCsF}(\Gamma) \tag{3.25}$$

$$\mathrm{jde}(\Gamma, \mathrm{Cs}) = \mathrm{kdG}(\Gamma) \tag{3.26}$$

Where A the area of the surface, Γ the surface concentration and Cs the concentration of the monomers at the subsurface and F, G are functions of the surface excess Γ. A crucial way to differentiate the use of each model is the dimensionless number Da which correlates the characteristic time for diffusion and adsorption.

$$\mathrm{Da} = \frac{\text{characteristic time for diffusion}}{\text{characteristic time for adsorption}} = \frac{\mathrm{tdif}}{\mathrm{tads}} \tag{3.27}$$

For values of $(\mathrm{Da} \ll 1)$ the process of adsorption consumes considerably more time and therefore kinetically limited. When $(\mathrm{Da} \gg 1)$ the process acting as a barrier is the diffusion and therefore considered as diffusion limited [8]. Diffusion limited models will not be studied in this thesis.

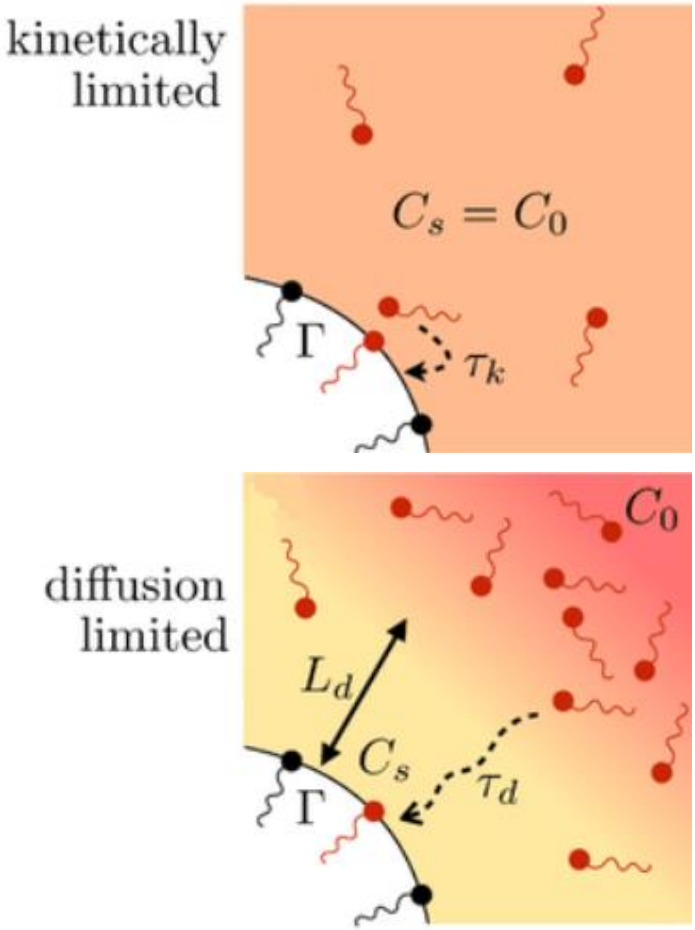

Figure 3.1: Representation of the kinetically and diffusion limited models [8].

3.4 Marangoni effects

The adsorption of monomers at an interface is not a symmetrical process and different surfactant concentrations depending on the location of the interface are established. In addition, surface rheology and surface compression and expansion are also factors that can alter the homogenous distribution of monomers on an interface. The phenomenon that offsets these disparities is driven by a surface tension gradient is called the Marangoni effect [19]. Inconsistencies in surfactant concentration produce shear stresses at any fluid interface, which are equal to the surface gradient of the surface tension. These stresses are called Marangoni stresses [8].

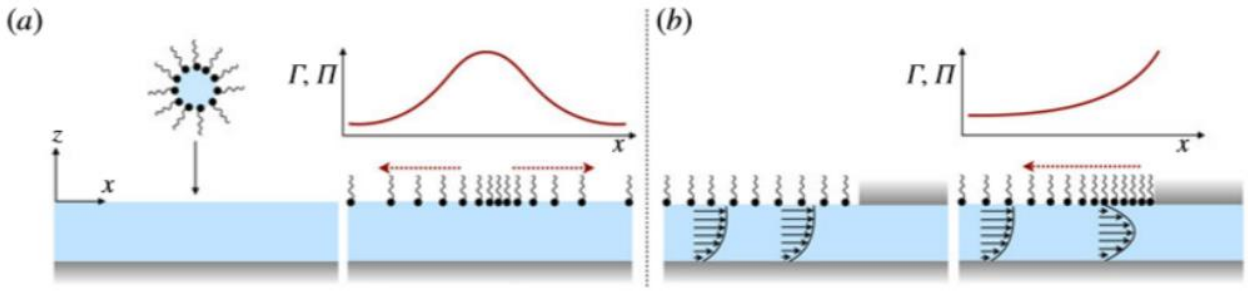

Figure 3.2: Two different examples of Marangoni flows induced by interfacial gradients of surface excess Γ [8]. (a) A local increase in surfactant concentration, (b) Surface compression due to flow.

3.5 Elasticity

The elasticity of an interface is an important property that describes deformations by the changes in the surface area. High values of elasticity are positive for the lung function since it is correlated with steeper changes of the surface tension [21]. When the surface coverage reaches a critical point where no more additional surfactants can enter the surface area, the limiting elasticity is obtained. The higher the elasticity of a surface the greater the resistance it opposes to changes [8]. The surface elasticity is vital for the normal function of the human lung due to its property of resisting to the collapse effect [20]. The Gibbs elasticity is defined as [21]:

$$\mathrm{E_G} = \frac{\mathrm{d}\Pi}{\mathrm{dLn}\Gamma} \tag{3.28}$$

3.6 Compressibility

At high frequency and at high concentration (close to saturation) the classic isotherms used to calculate the elasticity E of a monolayer fail to correlate with the experimental data and the values of E tend to reach unrealistically high values fig. 2.8 [22]. For this reason, the concept of compressibility was used. The forces of the surfactant molecules at high concentrations are forcing the molecules to occupy a smaller space hence reducing the minimum moral area of the surfactants Ω [23]. This can be observed by the tails of the molecules which tend to be perpendicular to the surface. The greater the angle of the tail and the surface the greater the compressibility [10], [22]. For reference the compression of the lung monolayer by the decreasing surface of the alveoli during exhalation can lead to values of surface tension σ of below 5 mn/m and even 1 mn/m [24]. Using this approach, the molar area of a surfactant is

affected by the surface pressure Π and the compressibility coefficient ε [23].

$$\Omega = \Omega_0(1 - \varepsilon\Pi) \tag{3.29}$$

Where Ω_0 is the moral area at zero surface pressure and ε is the surface compressibility. For a DPPC molecule at maximum tilt angle the surface coverage is about 0.42 nm^2/molecule at a surface pressure of 50 mN/m [10]. As the surface pressure increases and the surface concentration Γ approaches Γ_∞ the limiting elasticity E_0 is obtained [22].

$$E_0 = \frac{d\Pi}{dLn\Gamma} \approx \frac{1}{\varepsilon} \tag{3.30}$$

which shows a direct correlation of limiting elasticity with the intrinsic compressibility coefficient.

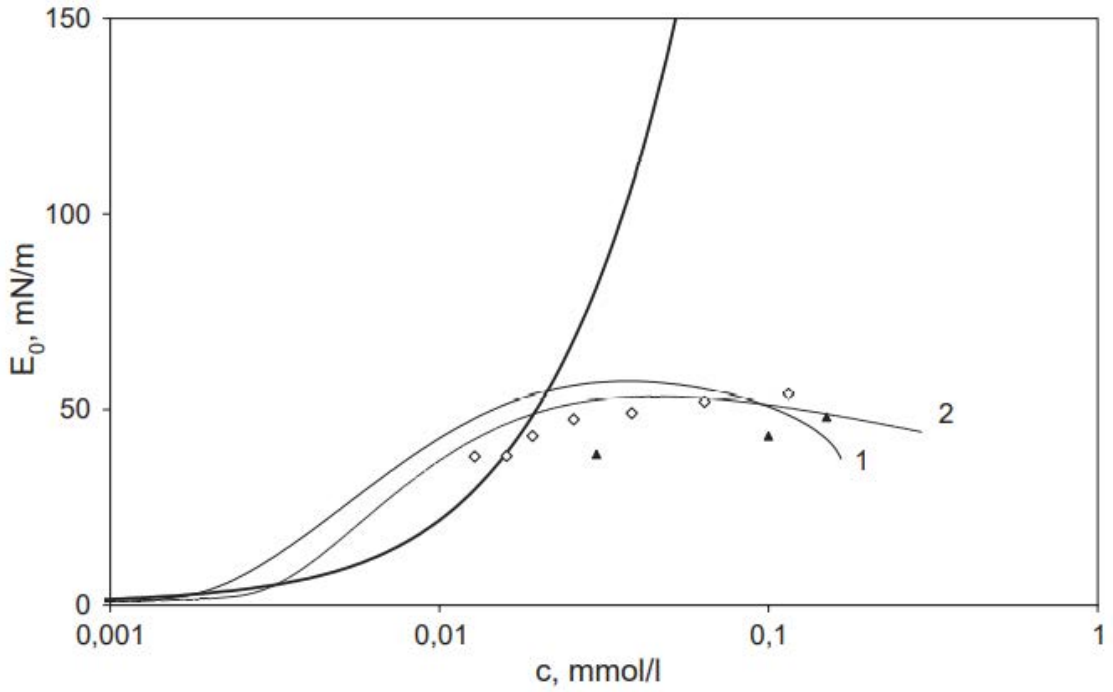

Figure 3.3: Limiting elasticity E_0 versus concentration using the Frumkin model (bold line) and models that account for the intrinsic compressibility (lines 1,2). Experimental data are shown as symbols [22].

3.7 Micelle formation

As a surface that contains surfactants is compressed or surfactant is being added at the solution, the surface concentration is increased until it reaches its maximum value of Γ_∞ and the moral area Ω cannot further decrease. At this point the compression of the surface or the addition of surfactant will not yield significant results for lowering the surface tension but will result in the formation of micelles. This point is the critical micelle concentration CMC. The

concentration of the pulmonary surfactant in the alveoli is above CMC and that affects the adsorption mechanism. The surfactants that are part of micelles need to break formation to be adsorbed to the surface and that can take intervals of 1 ms. For reference the deformation of a micelle can take up to several seconds. The micelles act as a reservoir of surfactants for the monolayer at the surface [25].

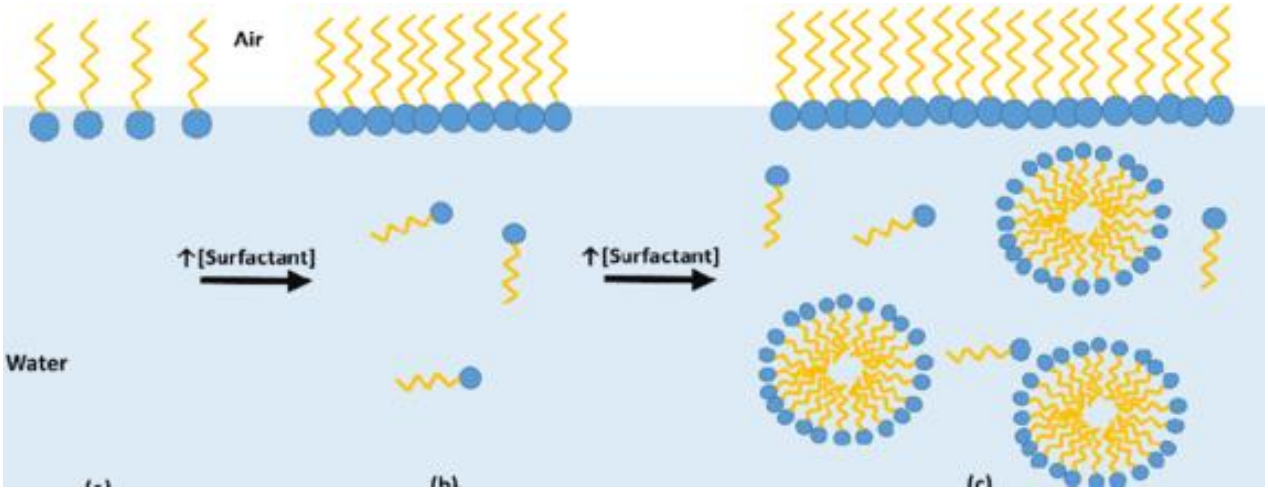

Figure 3.4: Micelle formation (Dantas et al.).

3.8 Collapse phenomenon

Another phenomenon that takes place at high surface concentrations is the collapse of the monolayer. When the interface of a system is reduced to a point that the surface pressure exceeds a limit Πc which depends on the composition of the surfactant and the conditions of the environment the 2-d structure of the monolayer is difficult to be preserved and 3-d structures are being formed. The way the 3-d structures are formed plays a key role in the reformation or reversibility (when possible) of the monolayer when the area is being expanded [14]. More analytically the collapse mechanisms are fracture, solubilization or squeeze out which are irreversible and folding which is reversible. The fracture mechanism usually takes place at very rigid monolayers and material is detached either in the subphase or in the air side of the interface by forming multilayered aggregates [14]. When a surfactant mixture which is composed from substances that have different collapse pressures πc the squeeze out mechanism is observed. As surface pressure is increased the substance with the lowest Πc is squeezed out of the monolayer which then is composed by the more stable components at high surface pressures [14]. The

synergistic interaction of the lung surfactant (mainly with the addition of SP-B) introduces a mechanism similar to the squeeze out mechanism but with the additional characteristic of reversibility. The monolayer is buckled and folded similar to how a piece of paper responds to lateral stresses [14]. When the surface pressure decreases (e.g., by increasing the surface area) the folded materials are reintroduced to the monolayer. This process is reversible and plays a key role in the fast reformation of the monolayer in the alveoli during inhalation.

Chapter 4. **PROBLEM SETUP**

The model formulation and solution is taken directly from article [21]. A single alveolus is modelled as a spherical domain consisting of a small volume, V that is periodically expanded and contracted (mimicking the inhalation and exhalation effect of a human lung), with surface area A that is in contact with air. The surfactant is modeled as a single active entity that resides in the form of vesicles in the bulk with constant concentration C and is adsorbed at the interface with surface concentration Γ. The domain is symmetrical and the surface concentration is also considered to be spatially uniform but changes with time as the volume changes and because of the tendency to reach equilibrium. The pulmonary surfactant layer is occupied predominantly by DPPC, thus the modelling of the surfactant can be achieved through a single component and the effect of the proteins on the DPPC is taken into account through parameters [10].

4.1 Equilibrium

Under equilibrium, adsorption is described by the Frumkin isotherm. The correlation of monomer bulk concentration C1 and the surface concentration of the monomers Γeq is achieved through the equation:

$$KC_1 = \exp(-2a\theta_{eq})\left(\frac{\Gamma eq}{\Gamma_\infty - \Gamma_{eq}}\right) = \exp(-2a\theta eq)\left(\frac{\theta_{eq}}{1-\theta_{eq}}\right) \quad (4.1)$$

Where a is a the Frumkin constant that expresses the attractive forces of the hydrophobic tails of the surfactant and the repulsive interactions of the water and surfactant molecules [25] and K the Frumkin adsorption constant. The pulmonary surfactant concentration in the alveoli far exceeds the critical micelle concentration C_{10}=10^{-9}-10^{-10} M. In this model the monomer concentration C_1 is equal to C_{10} since a higher concentration will have insignificant effect on the adsorption of monomers to the monolayer. Γ∞ is the saturated surface concentration where no more monomers can be adsorbed to the monolayer and θ=Γ/Γ∞ is the monolayer coverage.

The compressibility effect is also taken into consideration by using eq. (3.29). Using this approach, Γ∞ varies with surface pressure.

$$\Gamma_\infty = \frac{1}{\Omega} = \frac{1}{\Omega_0(1-\varepsilon\Pi)} \quad (4.2)$$

To calculate the surface tension on the surface, the equation of state is used that relates the

equilibrium surface tension σ_{eq} or surface pressure to the surface concentration using equation (2.2). The combination of the Frumkin isotherm (4.1) with the Gibbs equation eq. (3.11) and the compressibility effect (3.29) gives the equation of state.

$$\frac{\Pi\Omega_0}{RT}\left(1-\varepsilon\frac{\Pi}{2}\right) = -\ln(1-\theta) - \alpha\theta^2 \tag{4.3}$$

The changes in area of the surface of the alveoli due to compression and relaxation are accompanied by changes in the elasticity of the surface. The Gibbs elasticity is derived from eq. (4.3).

$$\frac{1}{E_G} = \left(-\frac{d\sigma}{dLn\Gamma}\right)^{-1} = \frac{\Omega_0}{RT}\frac{(1-\varepsilon\Pi)}{\left(\frac{\theta}{1-\theta} - 2a\theta^2\right)} + \frac{\varepsilon}{1-\varepsilon\Pi} \tag{4.4}$$

Eq. (4.4) represents two elasticity mechanisms in series, the first of which is compositional, i.e. related to variations in surface concentration, and the second is intrinsic, i.e. related to the surface compressibility of the monolayer.

4.2 Dynamics of the interface

The periodic changes of the interfacial area result in the change of the amount of adsorbed surfactant ΓA. This amount is affected by adsorption from the bulk, desorption to the bulk and exchange with a surfactant reservoir B. This results to the following equations

$$\frac{d(A\Gamma)}{dt} = A(j_{ads} - j_{des} + j_{ex}) \tag{4.5}$$

$$\frac{dB}{dt} = -Aj_{ex} \tag{4.6}$$

Where jads, jdes and jex correspond to surfactant transport by adsorption to the bulk, desorption to the bulk and exchange with the reservoir respectively.

The terms of equation (4.6) are being derived by the kinetics implied by the Frumkin isotherm,

$$\begin{aligned} j_{ads} - j_{des} &= k_{ads}C_{10}\,(\Gamma_\infty - \Gamma) - k_{des}\Gamma\exp(-2a\theta) \\ &= k_{ads}C_{10}[\,(\Gamma_\infty - \Gamma) - (\frac{\Gamma}{KC_{10}}\exp(-2a\theta))] \end{aligned} \tag{4.7}$$

Where k_{ads} is the adsorption rate constant and is influenced by the total concentration and composition of the surfactant [20] and C_{10} is the critical micelle concentration. The surfactant reservoir is being treated as a folded structure and therefore is ready for rapid replenishment of the monolayer during expansion. The forming of the three-dimensional structures takes effect

at when Π > Πmax, where Πmax is an input to the model. The maximum surface concentration Γmax is extracted by the equation of state (4.3) when Π ≥ Πmax and remains at this value even when further compression occurs. The surfactant that is removed during further compression is added to the reservoir B. The term jex describes the reverse of the folded 3d-structures. The content of B is reattached to the monolayer exclusively by this mechanism [21].

$$\mathrm{jex} = \mathrm{k_r}(\Gamma_\infty - \Gamma) \tag{4.8}$$

Where k_r is the constant of the re-insertion of surfactant from the reservoir.

4.3 Model formulation

The interfacial excess Γ is calculated by numerical integration of eqs (4.5)-(4.7) with initial conditions Γ(t = 0) = Γ_{eq} and B(t = 0) = 0. Depending on the state of Γ and B, the model takes different forms. Firstly, when Γ < Γ_{max} and B = 0 the interface can be either in compression or expansion, but the reservoir does not interact with the system and it is empty at all times. This situation is described by the following equations.

$$\frac{\mathrm{d}\Gamma}{\mathrm{dt}} = \mathrm{k_{ads}C_{10}}\left[\ (\Gamma_\infty\ - \Gamma) - \left(\frac{\Gamma}{\mathrm{KC_{10}}}\exp(-2\mathrm{a}\theta)\right)\right] - \frac{\Gamma}{\mathrm{A}}\frac{\mathrm{dA}}{\mathrm{dt}} \tag{4.9}$$

$$\frac{\mathrm{dB}}{\mathrm{dt}} = 0 \tag{4.10}$$

When Γ < Γ_{max} and B > 0, the content of B is being transferred to Γ according to the equations:

$$\frac{\mathrm{d}\Gamma}{\mathrm{dt}} = \mathrm{k_{ads}C_{10}}\left[\ (\Gamma_\infty\ - \Gamma) - \left(\frac{\Gamma}{\mathrm{KC_{10}}}\exp(-2\mathrm{a}\theta)\right)\right] - \frac{\Gamma}{\mathrm{A}}\frac{\mathrm{dA}}{\mathrm{dt}} + \mathrm{k_r}(\Gamma_\infty - \Gamma) \tag{4.11}$$

$$\frac{\mathrm{dB}}{\mathrm{dt}} = -\mathrm{Ak_r}(\Gamma_\infty - \Gamma) \tag{4.12}$$

When Γ = Γ_{max}, two possibilities emerge depending on whether there is an impulse for addition or removal of surfactant. Using the term J:

$$\mathrm{J} = \mathrm{k_{ads}C_{10}}\left[\ (\Gamma_\infty\ - \Gamma) - \left(\frac{\Gamma}{\mathrm{KC_{10}}}\exp(-2\mathrm{a}\theta)\right]\right. - \frac{\Gamma}{\mathrm{A}}\frac{\mathrm{dA}}{\mathrm{dt}} \tag{4.13}$$

For J ≥ 0 the interface is compressing and the surface pressure has exceeded the value needed

for collapse which leads to the addition of the excess surfactant to the reservoir B. During this phase the surface concentration remains constant at its maximum value.

$$\frac{d\Gamma}{dt} = 0 \tag{4.14}$$

$$\frac{dB}{dt} = AJ \tag{4.15}$$

The negative values of J signal the end of compression which is followed by the beginning of the expansion of the interface. For the instant that this statement is true the integrated system is as follows:

$$\frac{d\Gamma}{dt} = J \tag{4.16}$$

$$\frac{dB}{dt} = 0 \tag{4.17}$$

Lastly, the expansion of the interface leads to $\Gamma < \Gamma_{max}$ and the system is represented by the equations (4.9) and (4.10). The oscillation of the alveoli in the model is sinusoidal with a periodicity of 3 seconds as depicted in figure (4.1).

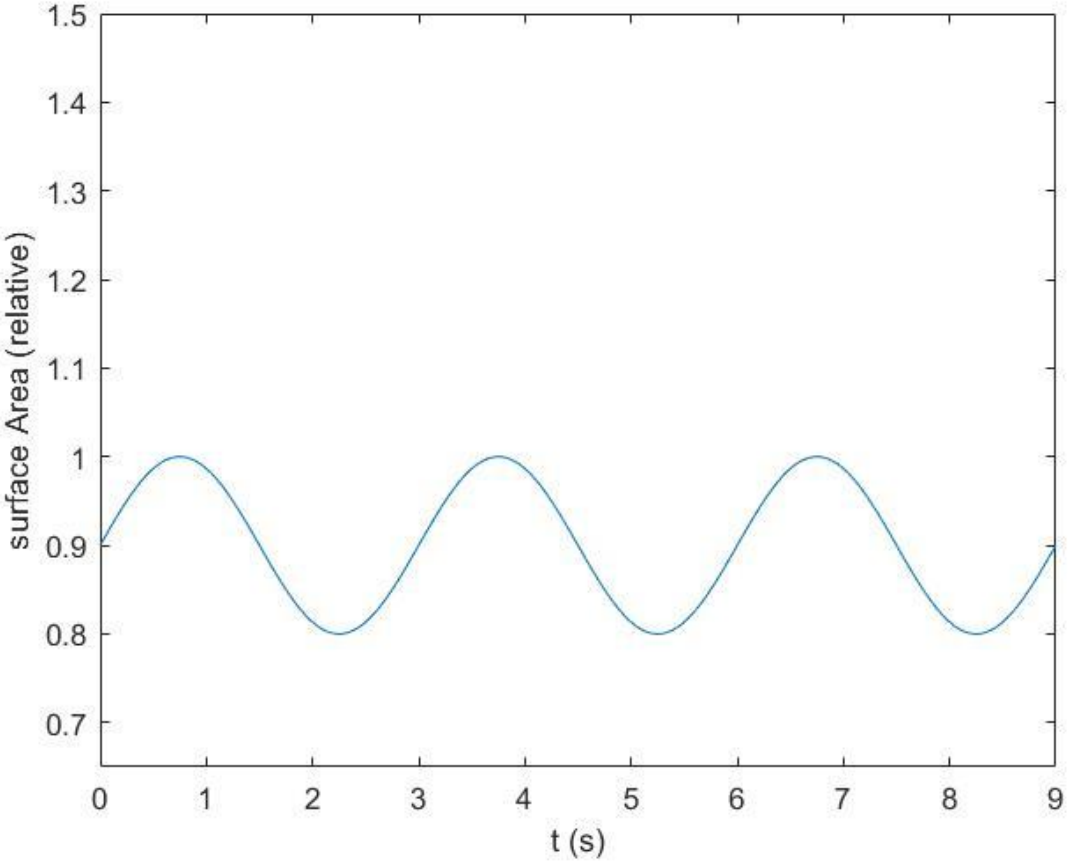

Figure (4.1): The oscillation of the alveoli's surface.

Chapter 5. **RESULTS**

The model was used to observe the effect of various parameters on the behavior of the surfactant under cyclic compression and expansion. The program used for these simulation is MATLAB. The variables that are adjusted are the equilibrium surface tension σ_{eq}, the compressibility ε, the parameter k_r, the Frumkin parameter a, the compression ratio dictated by the minimum surface area achieved Amin and the temperature of the solvent. Lastly the Runge-Kutta method was applied to observe differences of the model due to the iterative method used to solve the problem. The variables are adjusted having as reference the parameters used on [21] and all in all cases the air is humid with 100% relative humidity. The temperature and the Frumkin parameter are 37 °C and 0 respectively for all cases that do not investigate these parameters.

5.1 Equilibrium surface tension and compressibility coefficient

The effect of the equilibrium surface tension and the compressibility coefficient on the behavior of the surfactant is measured. The changes in surface tension, elasticity and surface excess are depicted in figures 5.1, 5.2, 5.3,5.4 with parameters as shown in table 5.1.

	σ_{min}(mN/m)	σ_{eq}(mN/m)	$k_{ads}C_{10}$(s^−1)	kr(s^−1)	ε(m/mN)	CR(%)
a	5	22	18	12	0.005	25
b	5	25	18	12	0.005	25
c	5	22	18	12	0.007	25
d	5	25	18	12	0.007	25

Table 5.1: Values of parameters for the equilibrium surface tension and compressibility coefficient case.

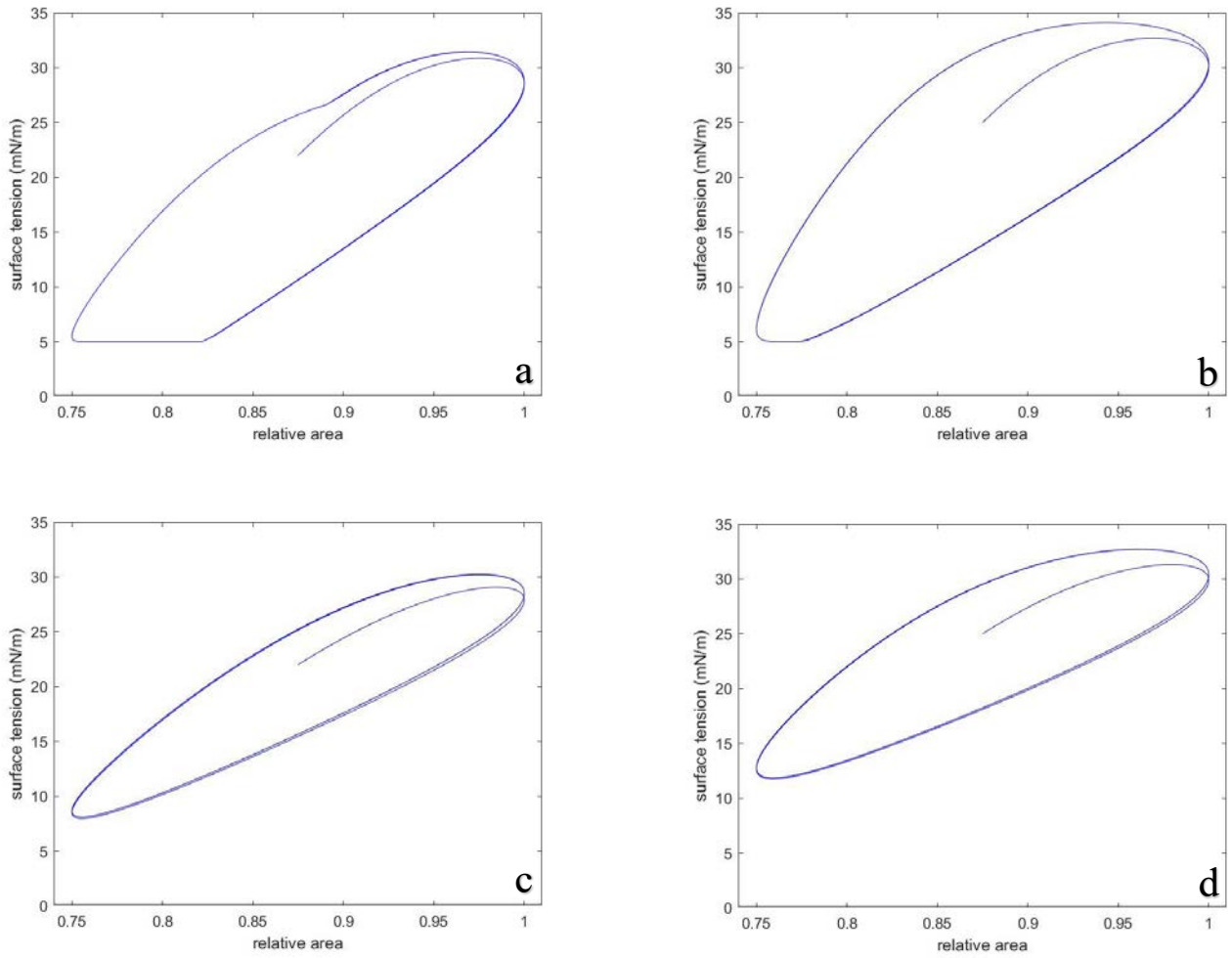

Figure 5.1: Surface tension (mN/m) versus relative area at an equilibrium surface tension of a) 22 mN/m (ε=0.005 m/mN, b) 25 (ε=0.005 m/mN), c) 22 mN/m (ε=0.007 m/mN) and d) 25 mN/m (ε=0.007 m/mN).

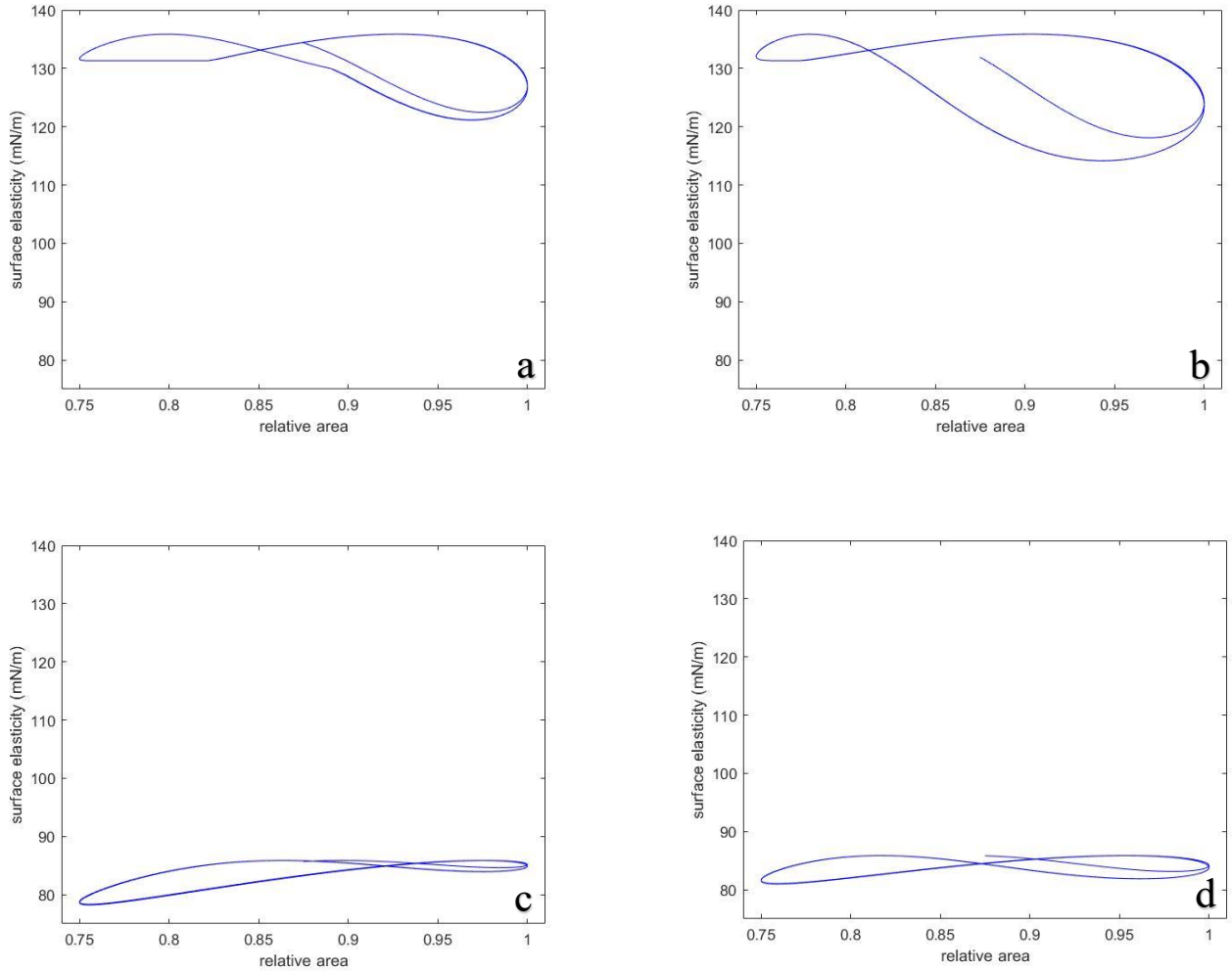

Figure 5.2: Surface elasticity (mN/m) versus relative area at equilibrium surface tension of a) 22 mN/m (ε=0.005 m/mN, b) 25 (ε=0.005 m/mN), c) 22 mN/m (e=0.007 m/mN) and d) 25 mN/m (e=0.007 m/mN).

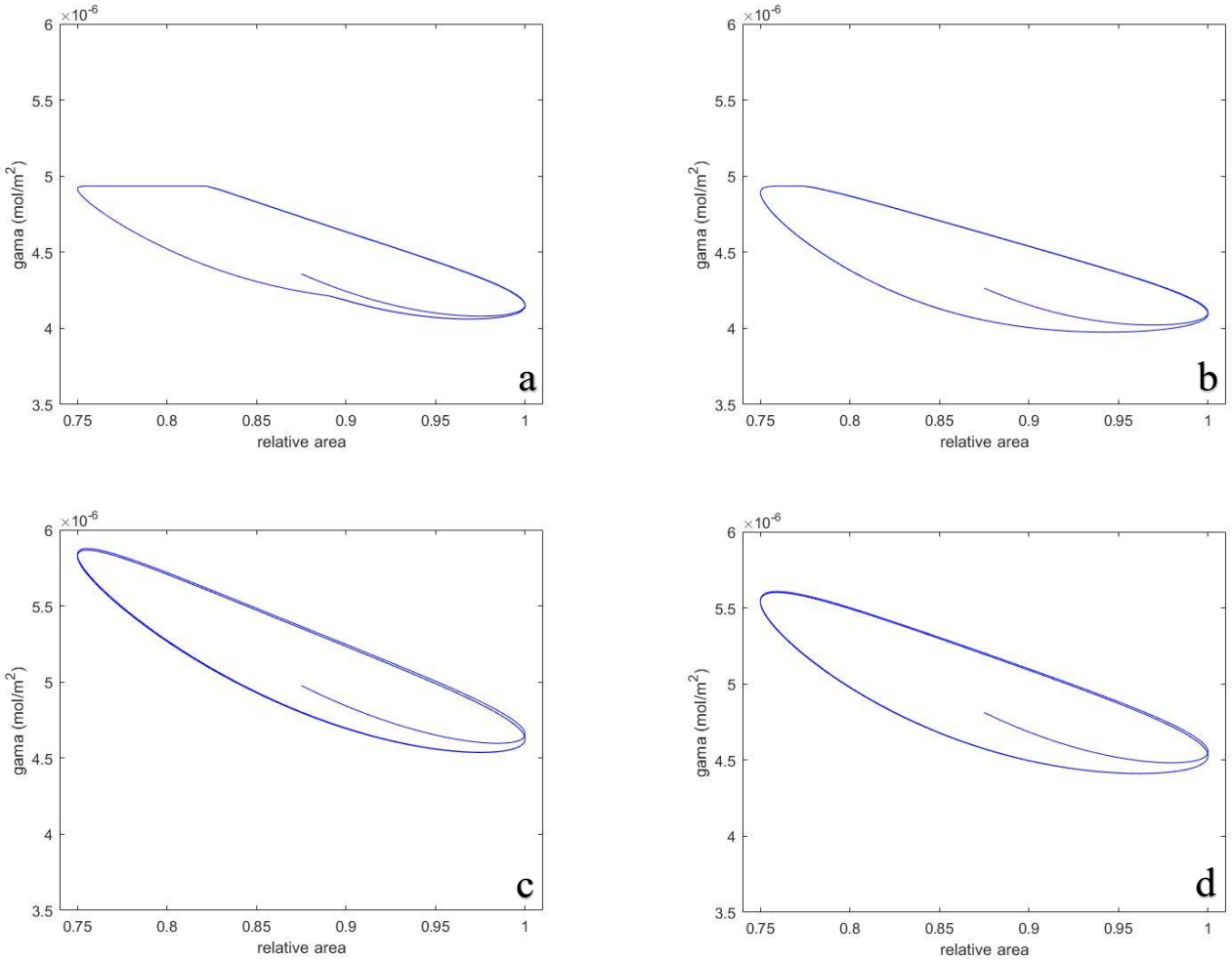

Figure 5.3: Interfacial excess (mol/m2) versus relative area at equilibrium surface tension of a) 22 mN/m (ε=0.005 m/mN, b) 25 (ε=0.005 m/mN), c) 22 mN/m (e=0.007 m/mN) and d) 25 mN/m (e=0.007 m/mN).

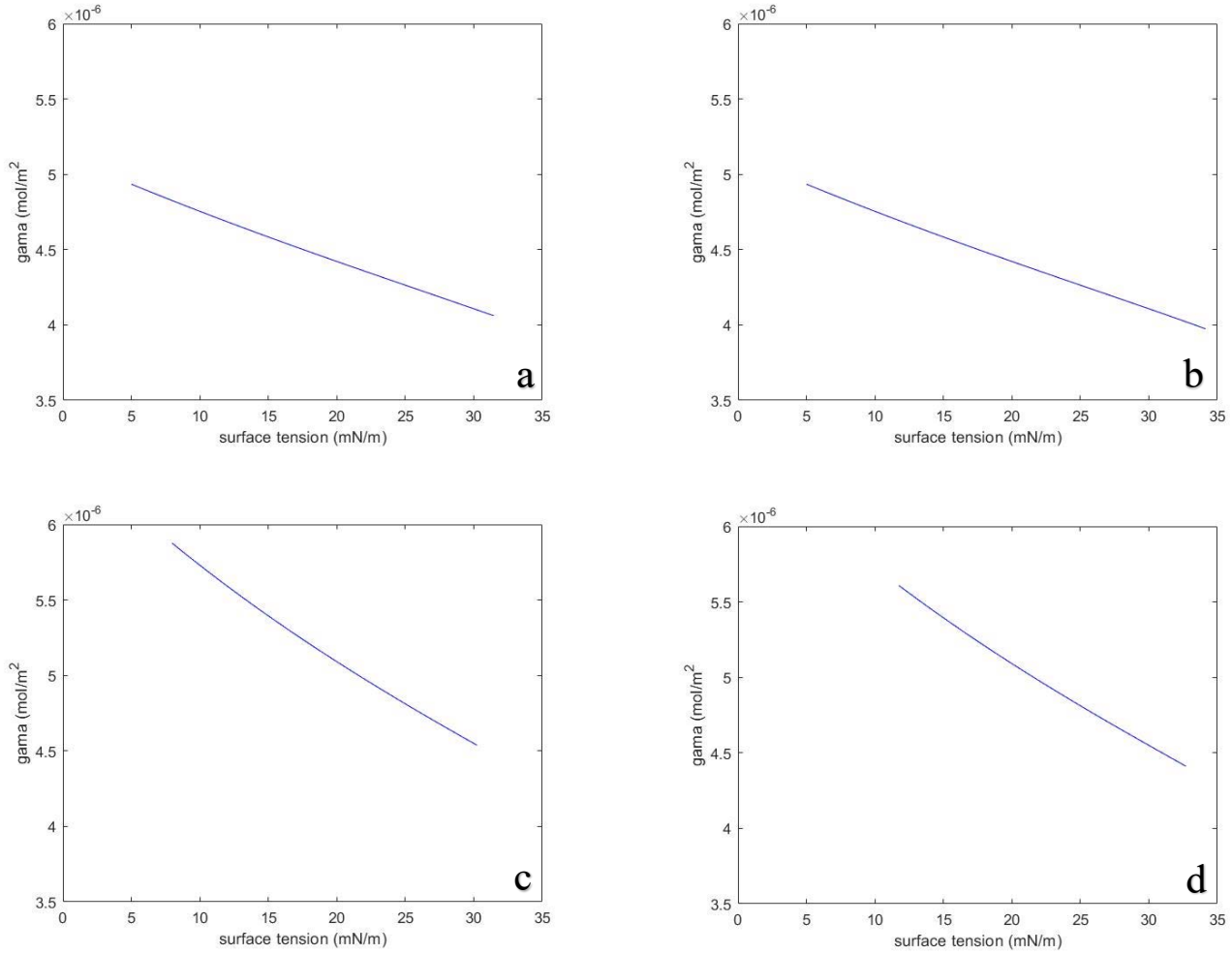

Figure 5.4: Interfacial excess (mol/m2) versus surface tension (mN/m) at equilibrium surface tension of a) 22 mN/m (ε=0.005 m/mN, b) 25 (ε=0.005 m/mN), c) 22 mN/m (e=0.007 m/mN) and d) 25 mN/m (e=0.007 m/mN).

5.2 Frumkin parameter

The effect of the Frumkin parameter on the behavior of the surfactant is measured for two different cases. For the first case the changes in surface tension, elasticity and surface excess are depicted in figures 5.5, 5.6, 5.7, 5.8 with parameters as shown in table 5.2 and figures 5.9, 5.10, 5.11, 5.12 correspond to the second case with parameters as shown in table 5.3.

Case 1	σ_{min}(mN/m)	σ_{eq}(mN/m)	$k_{ads}C_{10}$(s^−1)	kr(s^−1)	ε(m/mN)	CR(%)	Frumkin (a)
a	5	24	13	12	0.0051	20	0
b	5	24	13	12	0.0051	20	0.2
c	5	24	13	12	0.0051	20	0.5
d	5	24	13	12	0.0051	20	0.8

Table 5.2: Values of parameters for the Frumkin parameter case (first case).

Case 2	σ_{min}(mN/m)	σ_{eq}(mN/m)	$k_{ads}C_{10}$(s^−1)	kr(s^−1)	ε(m/mN)	CR(%)	Frumkin (a)
a	12	24.5	35	12	0.0051	23.1	0
b	12	24.5	35	12	0.0051	23.1	0.2
c	12	24.5	35	12	0.0051	23.1	0.5
d	12	24.5	35	12	0.0051	23.1	0.8

Table 5.3: Values of parameters for the Frumkin parameter case (second case).

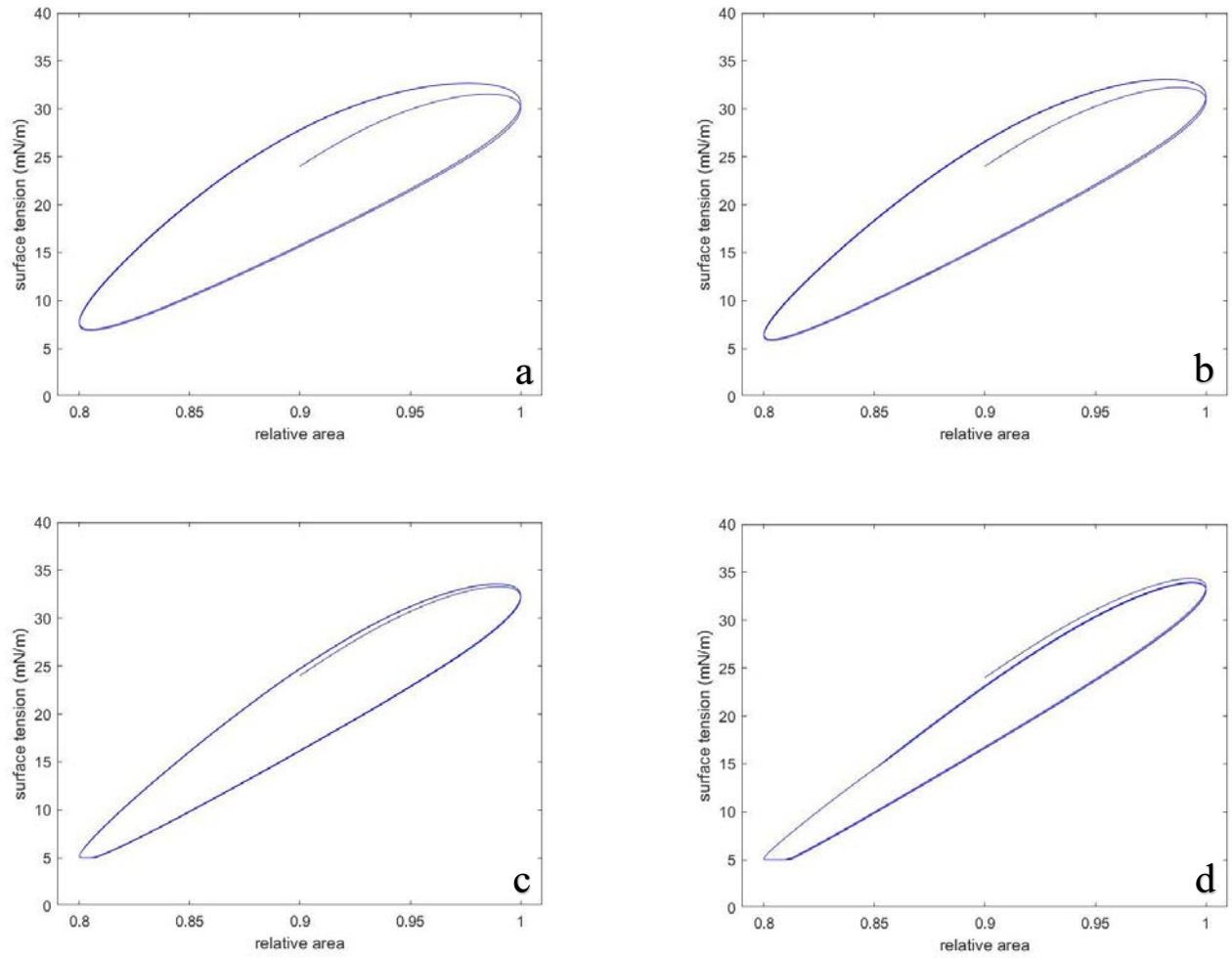

Figure 5.5: Surface tension (mN/m) versus relative area with values of the Frumkin parameter a of a) 0, b) 0.2, c) 0.5 and d) 0.8 (first case).

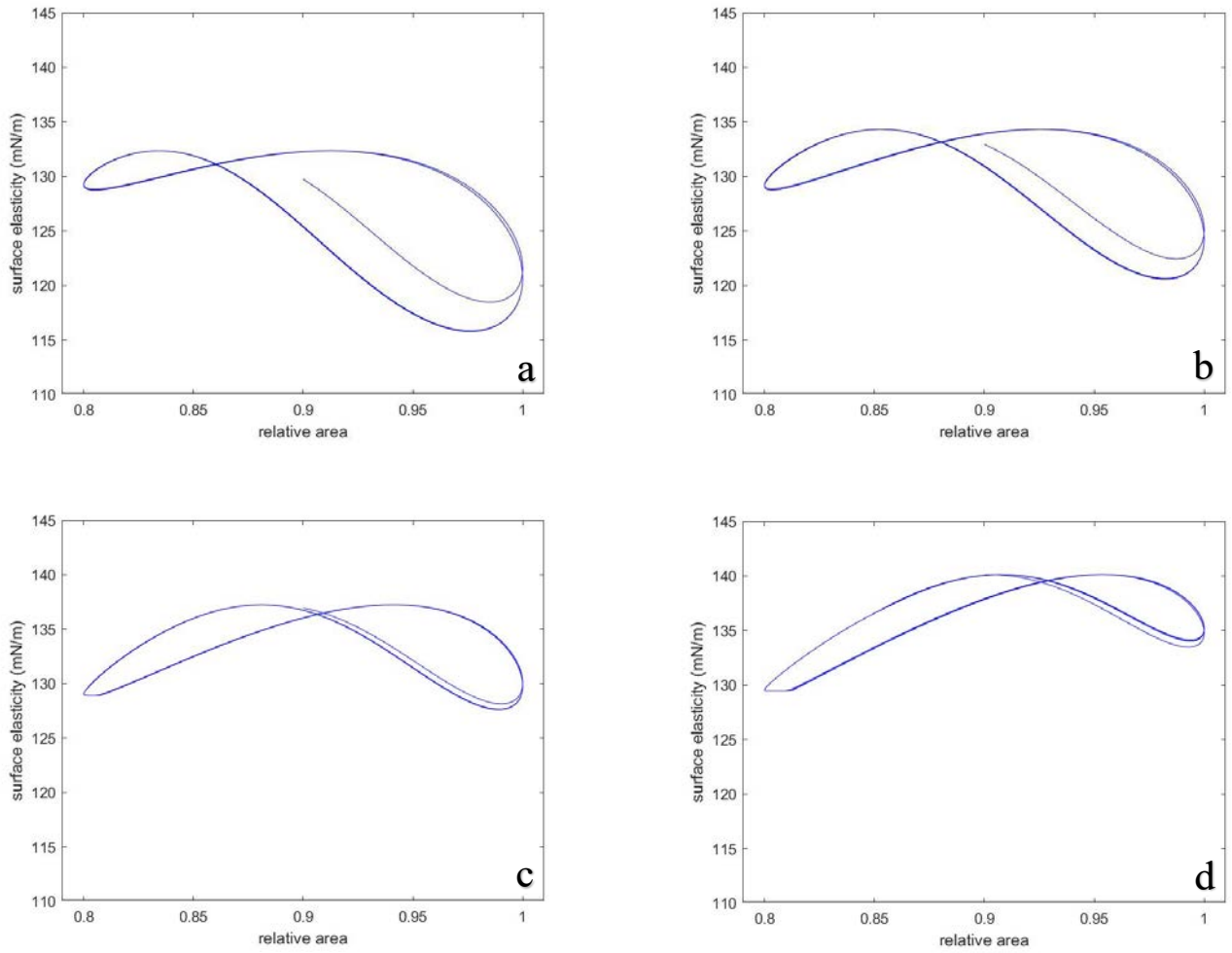

Figure 5.6: Surface elasticity (mN/m) versus relative area with values of the Frumkin parameter a of a) 0, b) 0.2, c) 0.5 and d) 0.8 (first case).

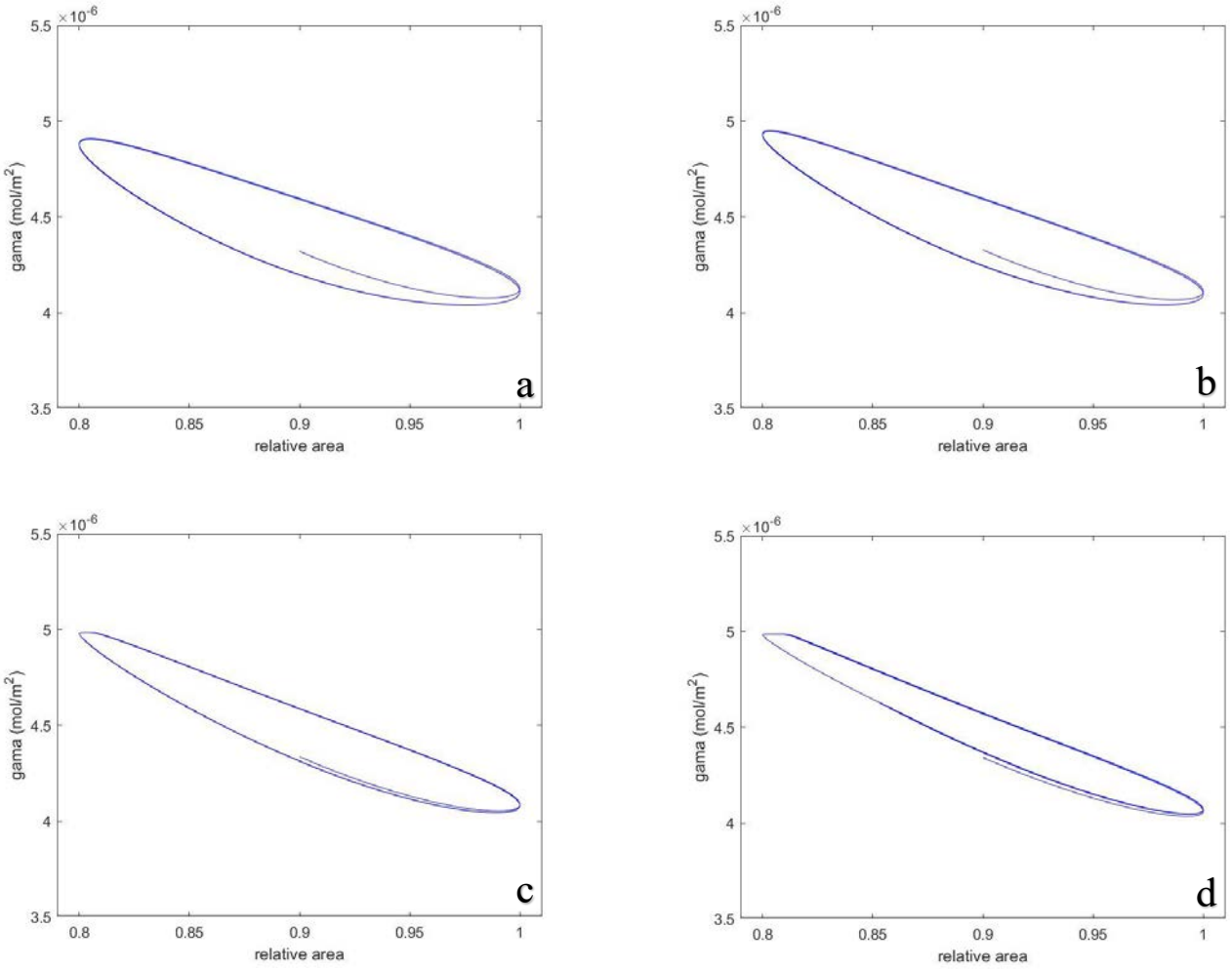

Figure 5.7: Interfacial excess (mol/m2) versus relative area with values of the Frumkin parameter a of a) 0, b) 0.2, c) 0.5 and d) 0.8 (first case).

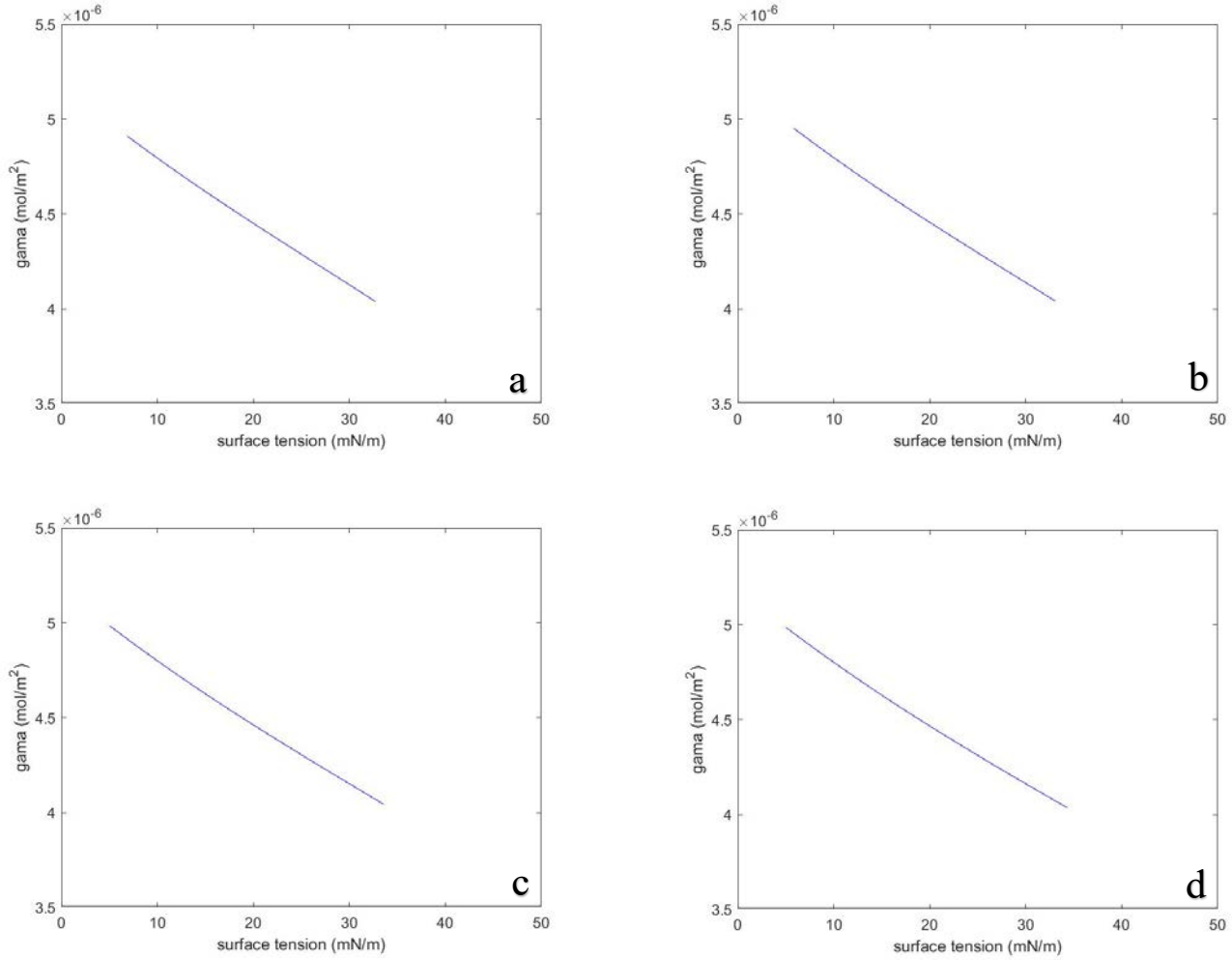

Figure 5.8: Interfacial excess (mol/m2) versus surface tension (mN/m) with values of the Frumkin parameter a of a) 0, b) 0.2, c) 0.5 and d) 0.8 (first case).

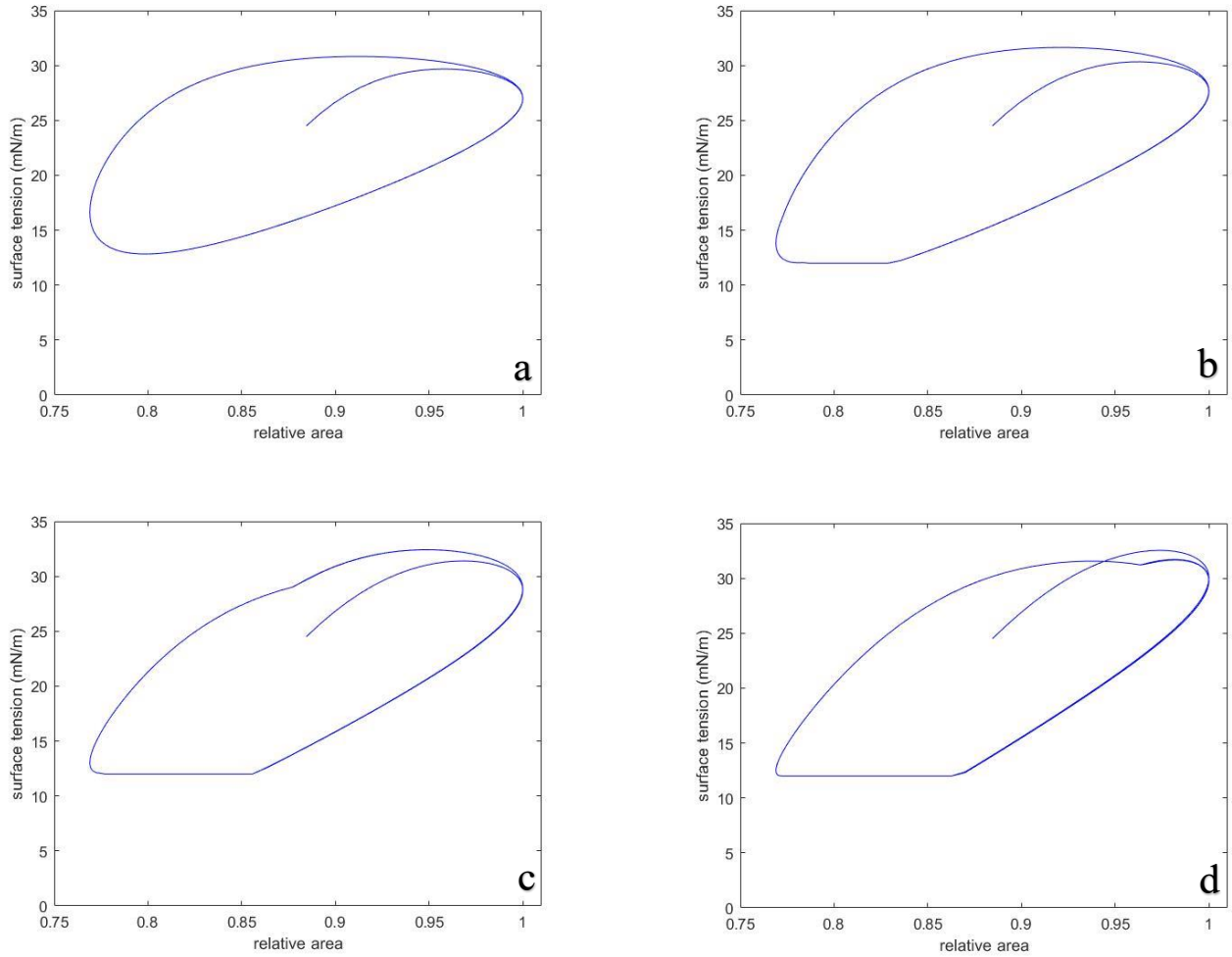

Figure 5.9: Surface tension (mN/m) versus relative area with values of the Frumkin parameter a of a) 0, b) 0.2, c) 0.5 and d) 0.8 (second case).

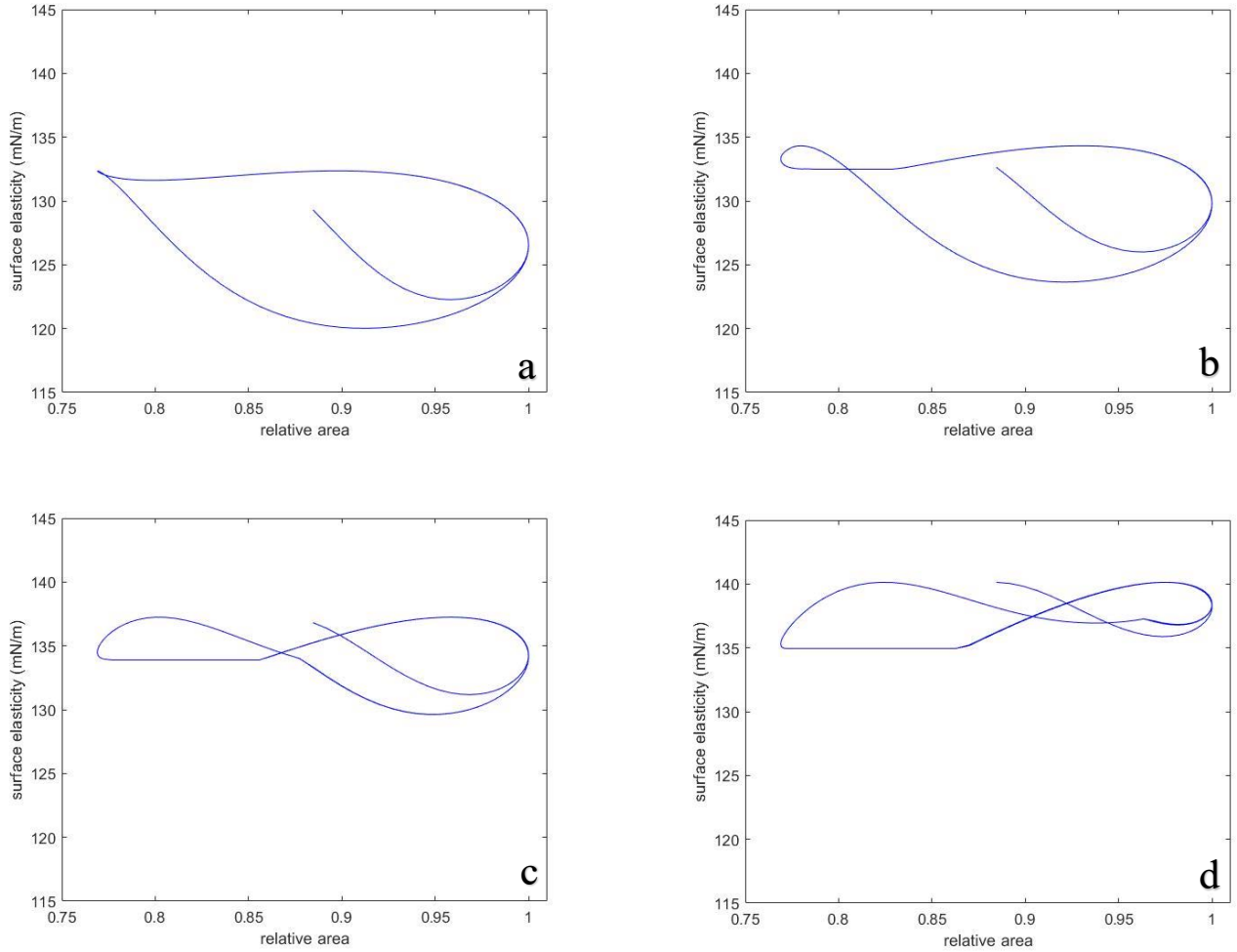

Figure 5.10: Surface elasticity (mN/m) versus relative area with values of the Frumkin parameter a of a) 0, b) 0.2, c) 0.5 and d) 0.8 (second case).

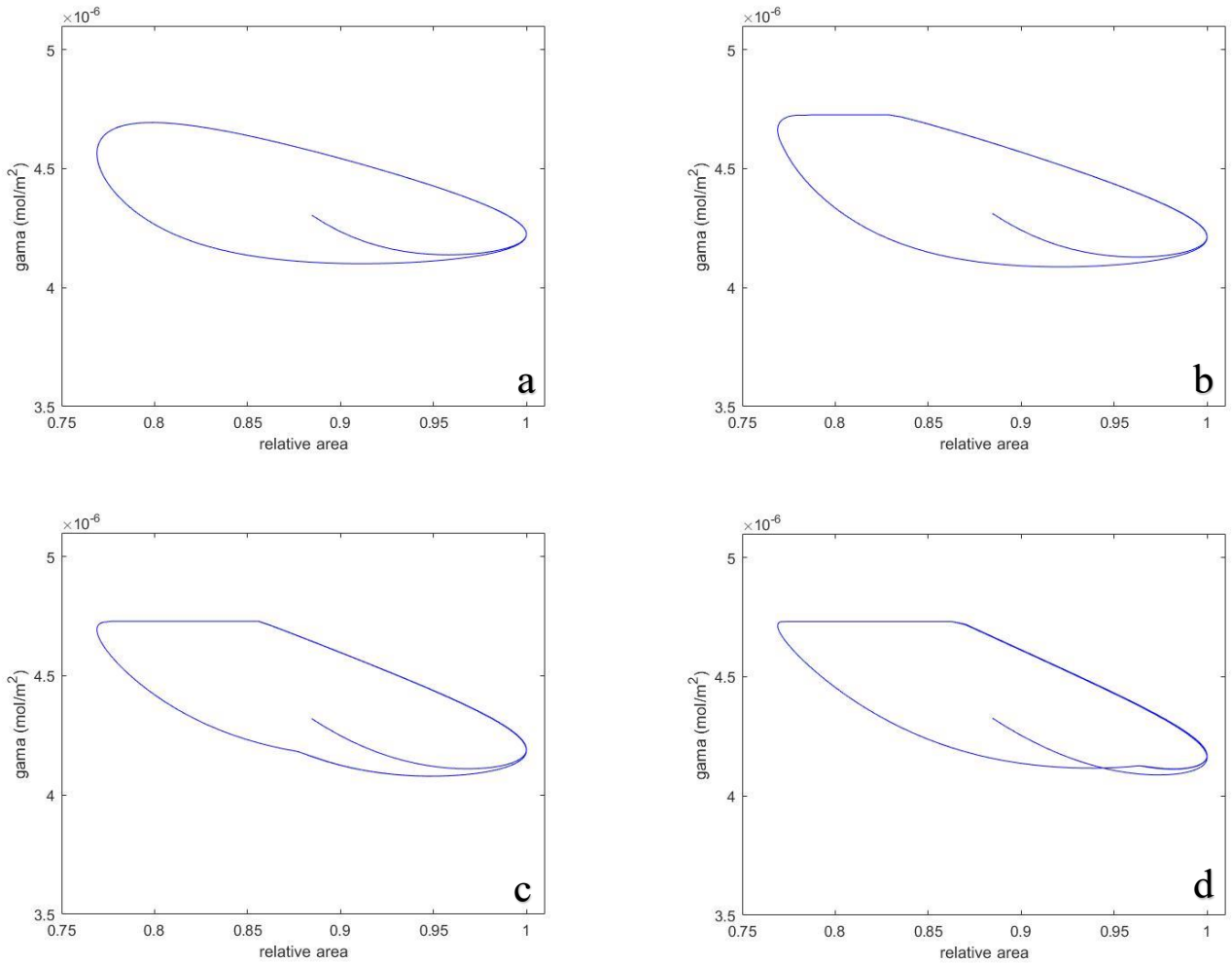

Figure 5.11: Interfacial excess (mol/m2) versus relative area with values of the Frumkin parameter a of a) 0, b) 0.2, c) 0.5 and d) 0.8 (second case).

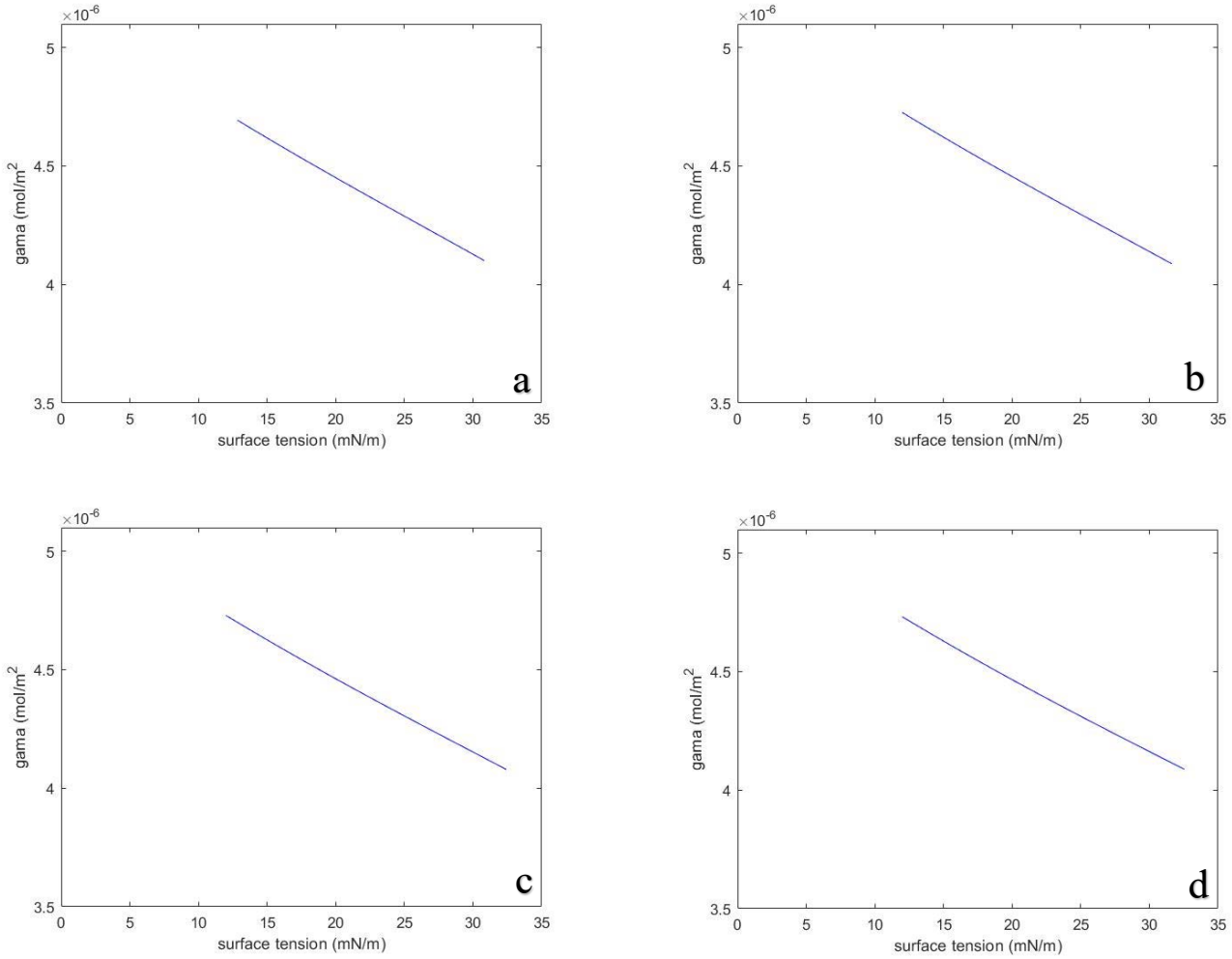

Figure 5.12: Interfacial excess (mol/m2) versus surface tension (mN/m) with values of the Frumkin parameter a of a) 0, b) 0.2, c) 0.5 and d) 0.8 (second case).

5.3 Kr parameter

The effect of the Kr parameter on the behavior of the surfactant is measured. The changes in surface tension, elasticity and surface excess are depicted in figures 5.13, 5.14, 5.15,5.16 with parameters as shown in table 5.4.

	σ_{min}(mN/m)	σ_{eq}(mN/m)	$k_{ads}C_{10}$(s^−1)	kr(s^−1)	ε(m/mN)	CR(%)
a	5	24	18	10	0.0051	25
b	5	24	18	14	0.0051	25
c	5	24	18	10	0.0051	30
d	5	24	18	14	0.0051	30

Table 5.4: Values of parameters for the Kr parameter case.

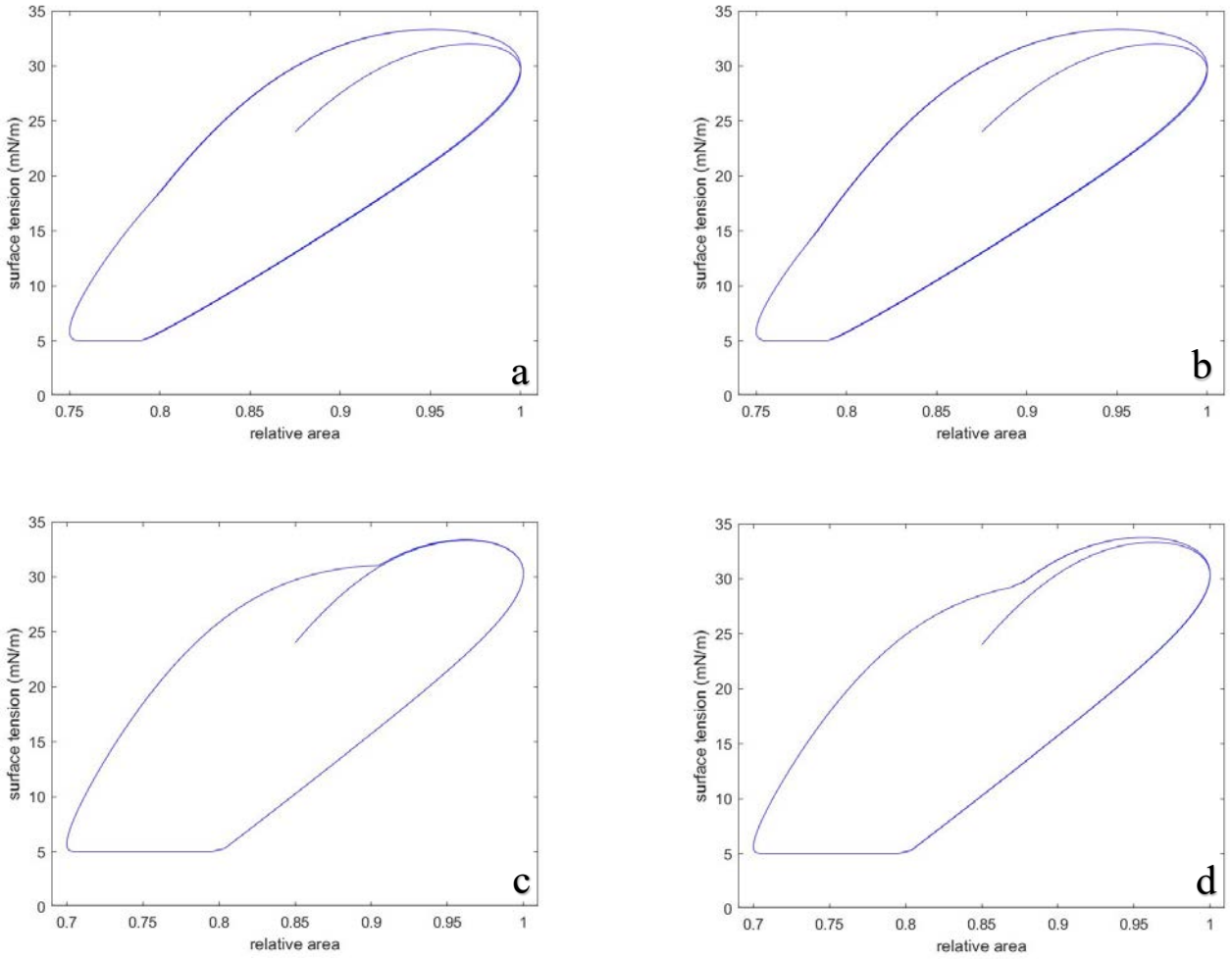

Figure 5.13: Surface tension (mN/m) versus relative area with values of the Kr parameter of a) 10, b) 14, c) 10 and d) 14.

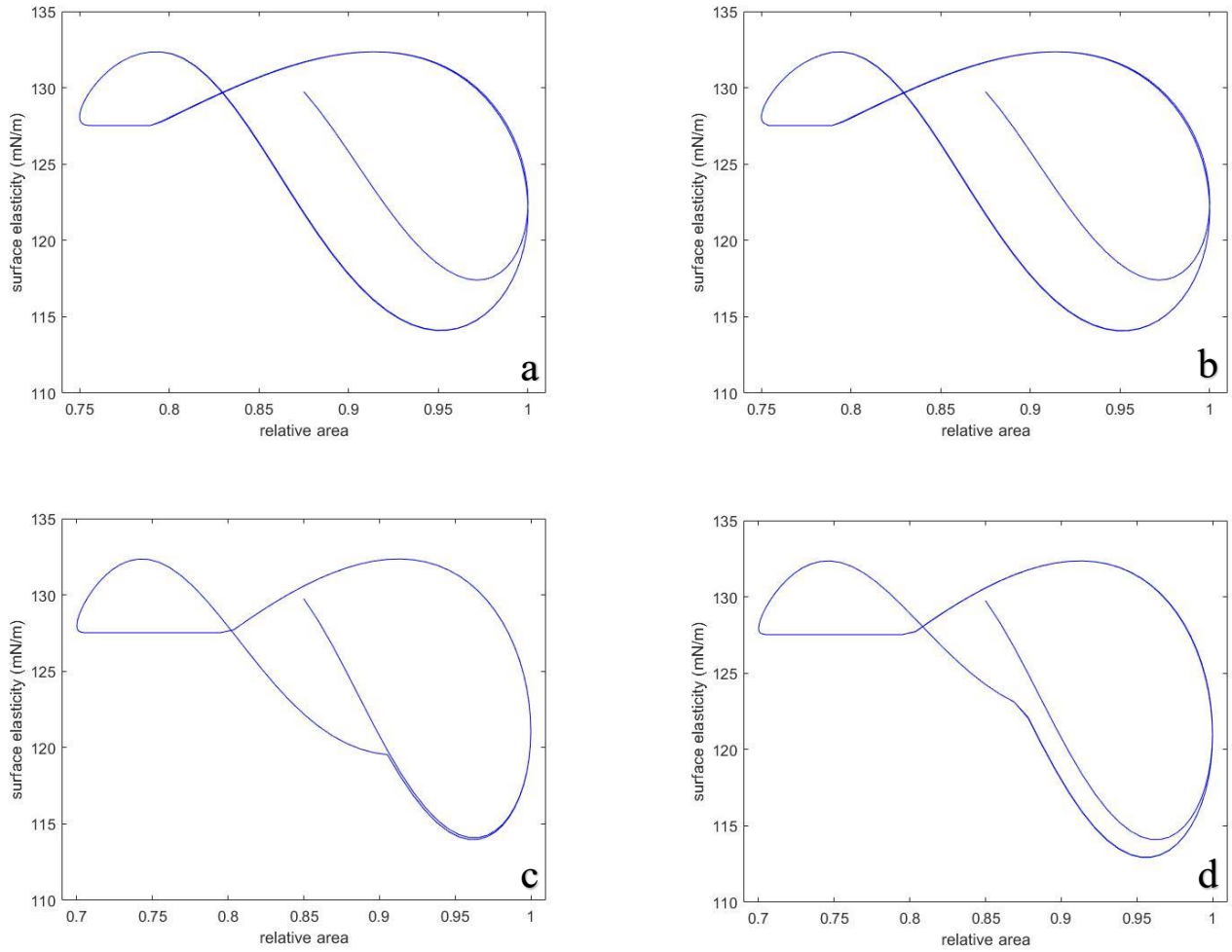

Figure 5.14: Surface elasticity (mN/m) versus relative area with values of the Kr parameter of a) 10, b) 14, c) 10 and d) 14.

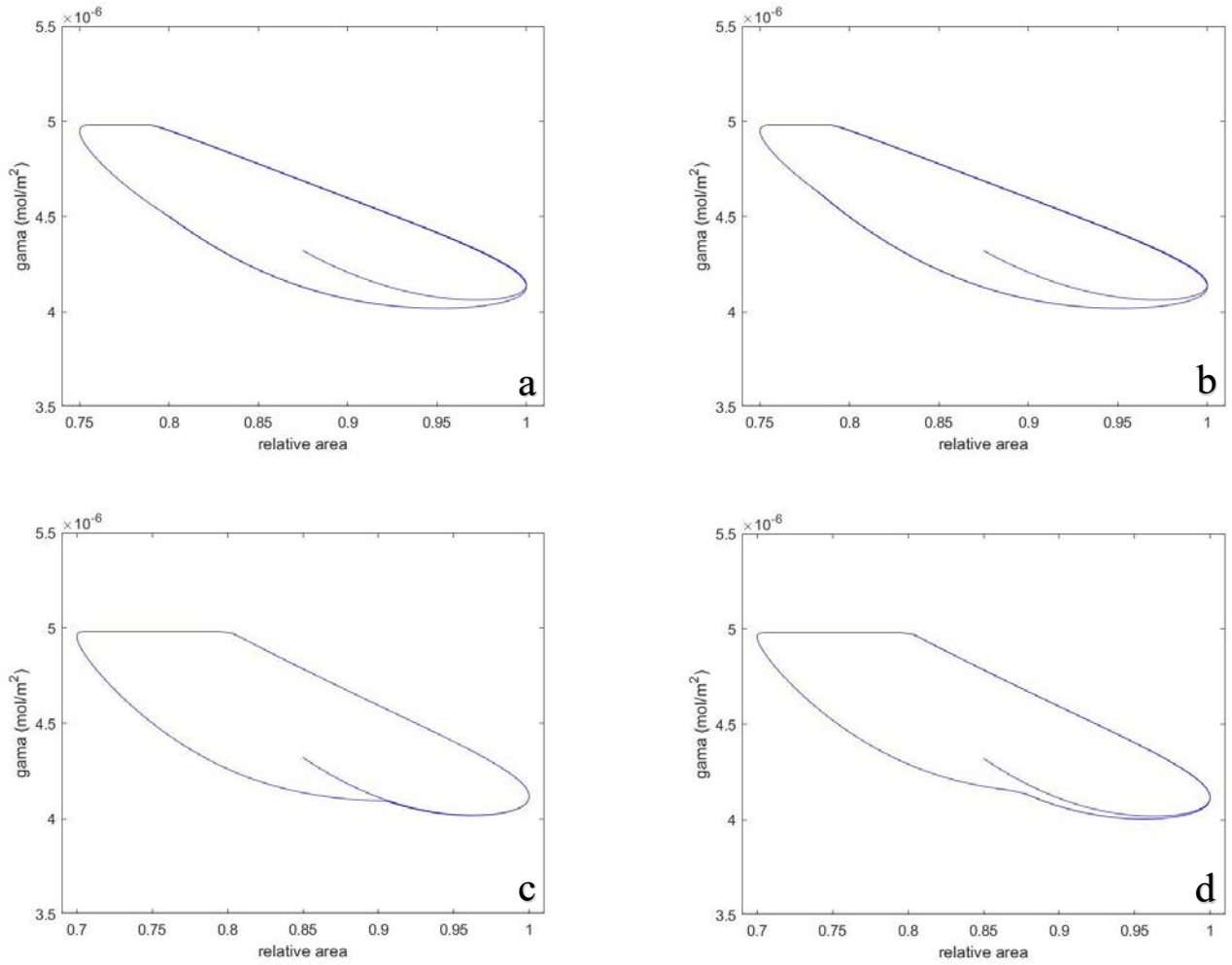

Figure 5.15: Interfacial excess (mol/m2) versus relative area with values of the Kr parameter of a) 10, b) 14, c) 10 and d) 14.

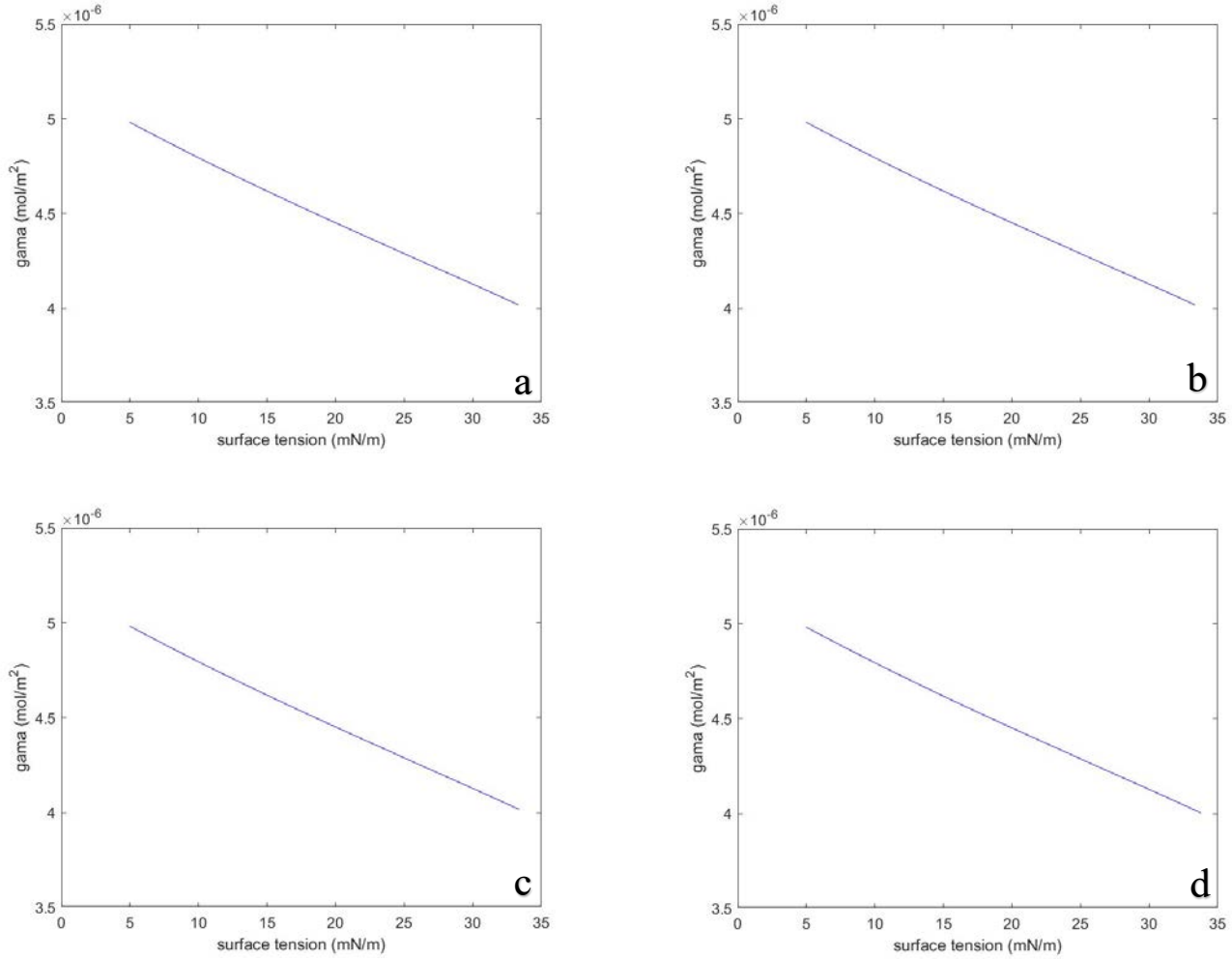

Figure 5.16: Interfacial excess (mol/m2) versus surface tension (mN/m) with values of the Kr parameter of a) 10, b) 14, c) 10 and d) 14.

5.4 Temperature

The effect of the temperature on the behavior of the surfactant is measured for 2 different cases. The changes in surface tension, elasticity and surface excess are depicted in figures 5.17, 5.18, 5.19, 5.20 with parameters as shown in table 5.5.

	σ_{min}(mN/m)	σ_{eq}(mN/m)	$k_{ads}C_{10}$(s^−1)	kr(s^−1)	ε(m/mN)	CR(%)	Temperature(°C)
a	5	24	13	12	0.0051	20	20
b	5	24	13	12	0.0051	20	40
c	12	24.5	35	12	0.0051	23.1	20
d	12	24.5	35	12	0.0051	23.1	40

Table 5.5: Values of parameters for the temperature parameter case.

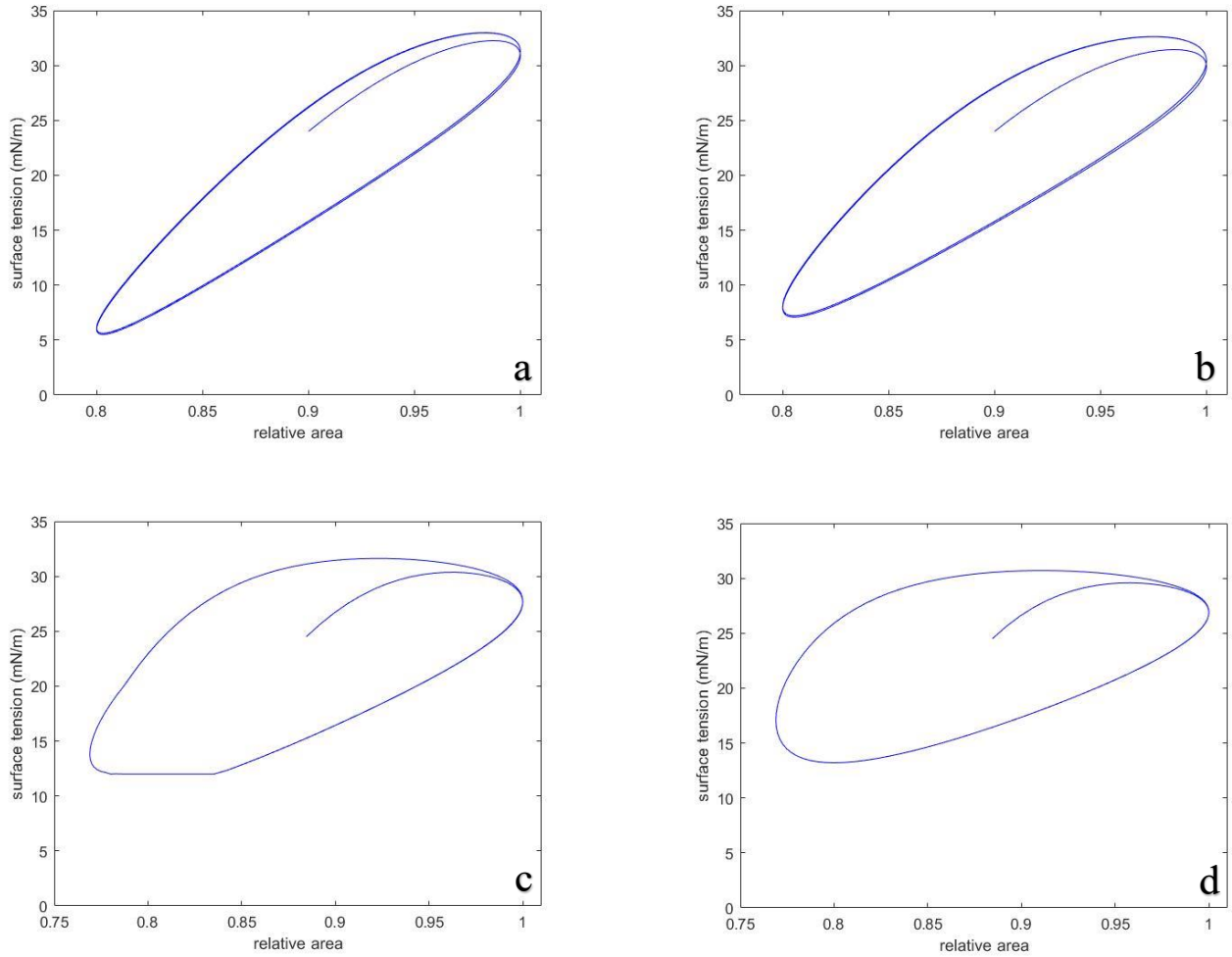

Figure 5.17: Surface tension (mN/m) versus relative area at the temperature of a) 20, b) 40, c) 20 and d) 40.

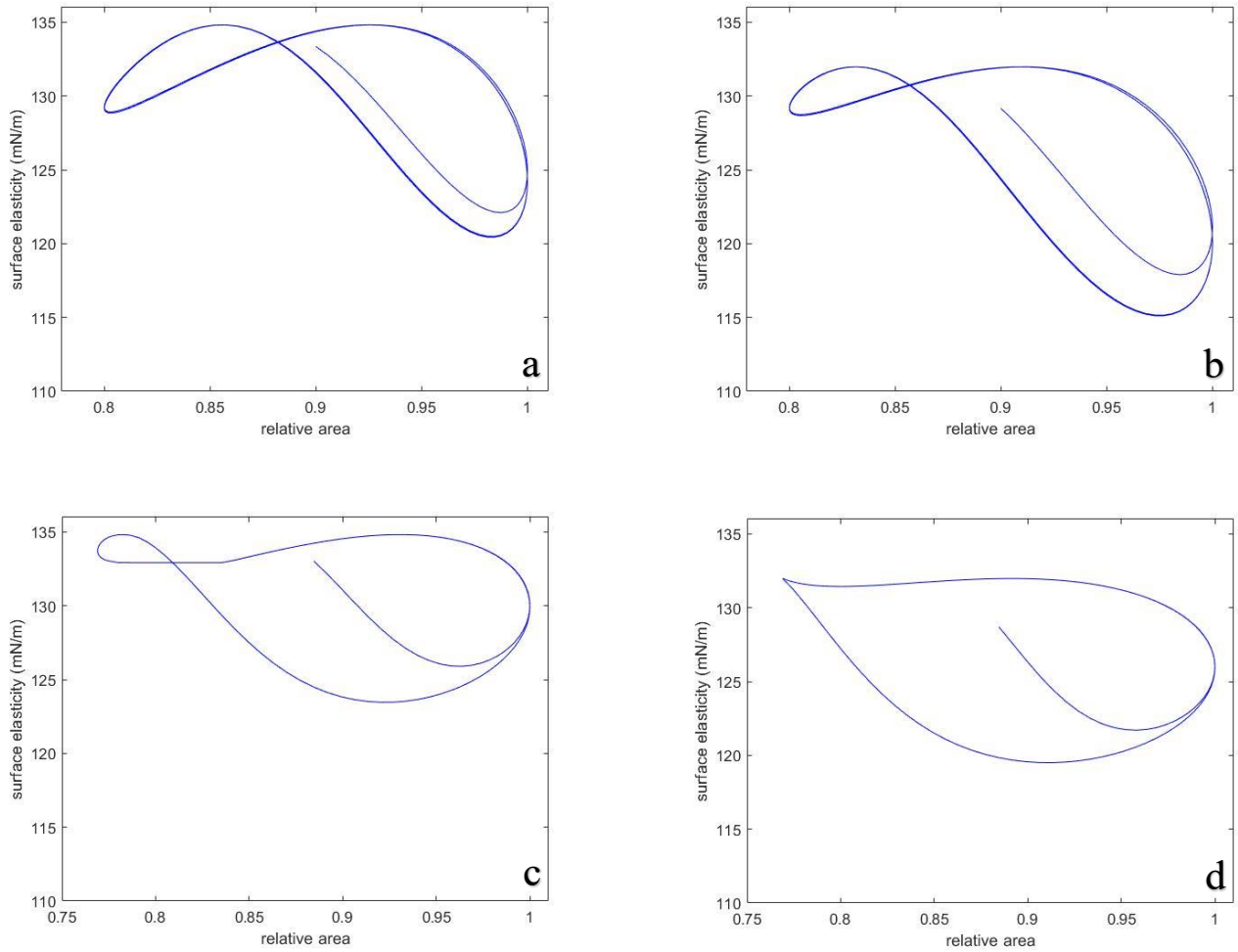

Figure 5.18: Surface elasticity (mN/m) versus relative area at the temperature of a) 20, b) 40, c) 20 and d) 40.

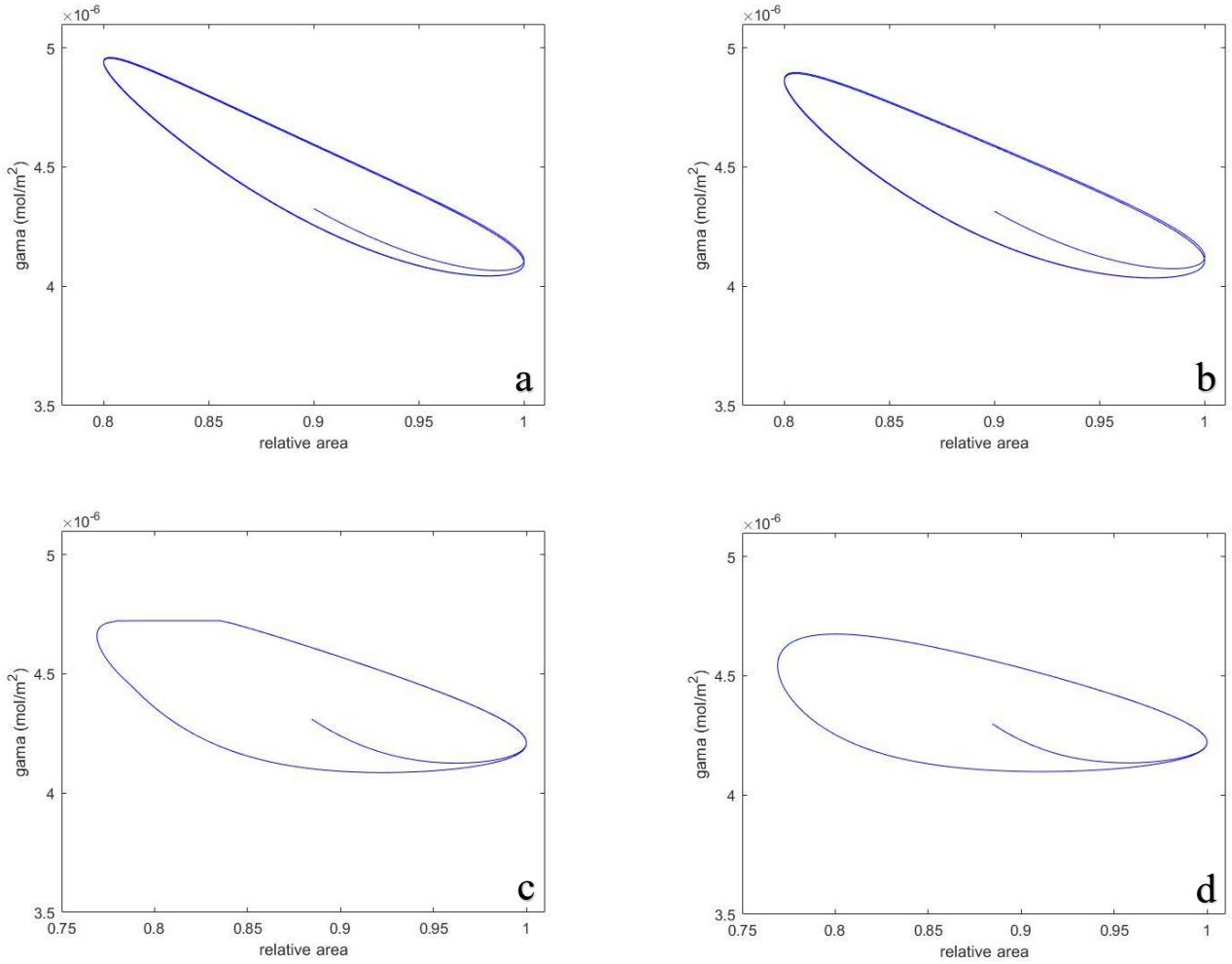

Figure 5.19: : Interfacial excess (mol/m2) versus relative area at the temperature of a) 20, b) 40, c) 20 and d) 40.

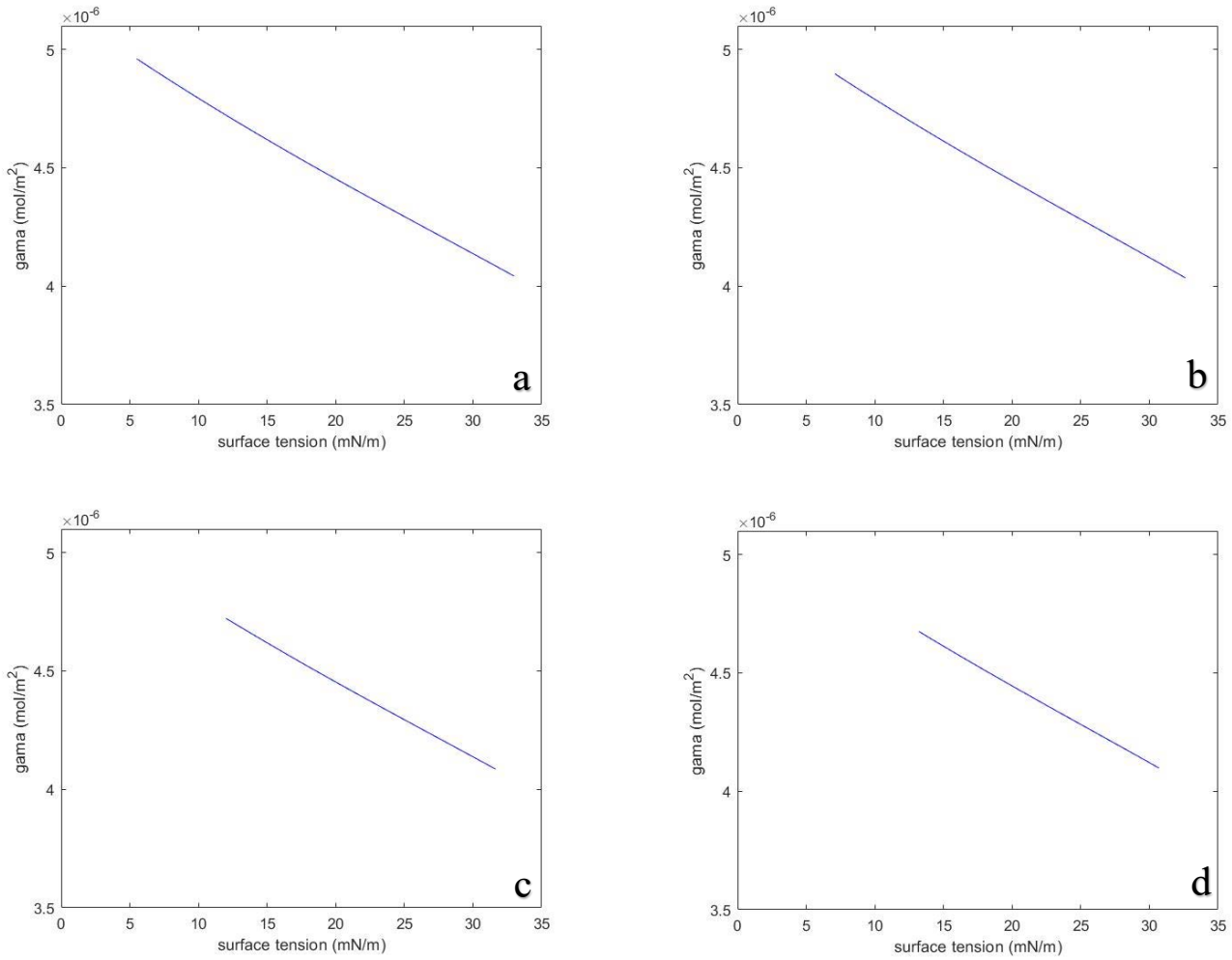

Figure 5.20: Interfacial excess (mol/m2) versus surface tension (mN/m) at the temperature of a) 20, b) 40, c) 20 and d) 40.

5.5 Compression ratio

The effect of the temperature on the behavior of the surfactant is measured for 2 different cases. The changes in surface tension, elasticity and surface excess are depicted in figures 5.21, 5.22, 5.23, 5.24 with parameters as shown in table 5.6.

	σ_{min}(mN/m)	σ_{eq}(mN/m)	$k_{ads}C_{10}$(s^−1)	kr(s^−1)	ε(m/mN)	CR(%)
a	5	24	10	16	0.0051	10
b	5	24	10	16	0.0051	20
c	5	24	10	16	0.0051	30
d	5	24	10	16	0.0051	40
e	5	24	10	16	0.0051	50
f	5	24	10	16	0.0051	60

Table 5.6: Values of parameters for the compression ratio parameter case.

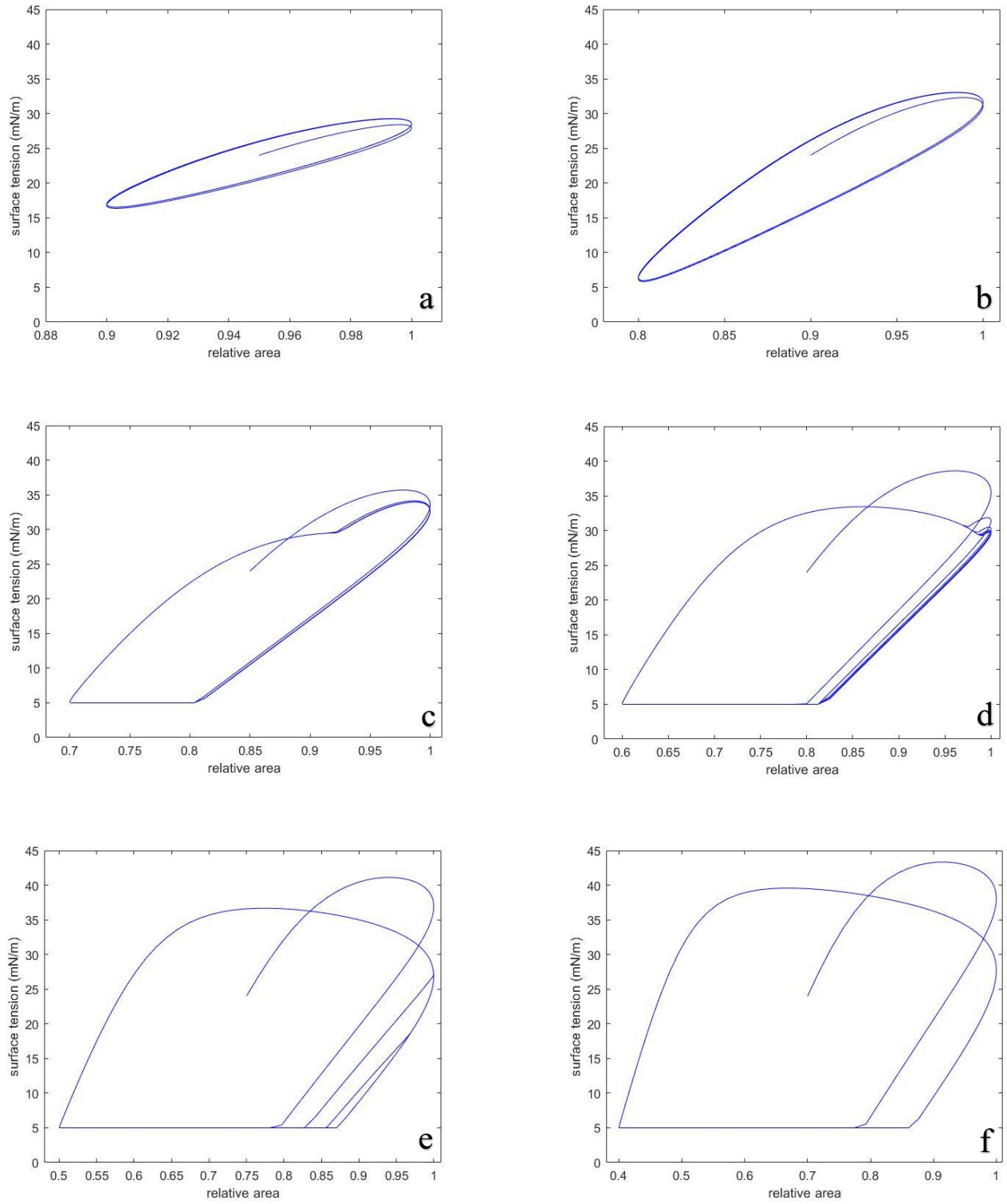

Figure 5.21: Surface tension (mN/m) versus relative area at a compression ratio of a) 10%, b) 20%, c) 30% ,40%d), e) 50% and f) 60%.

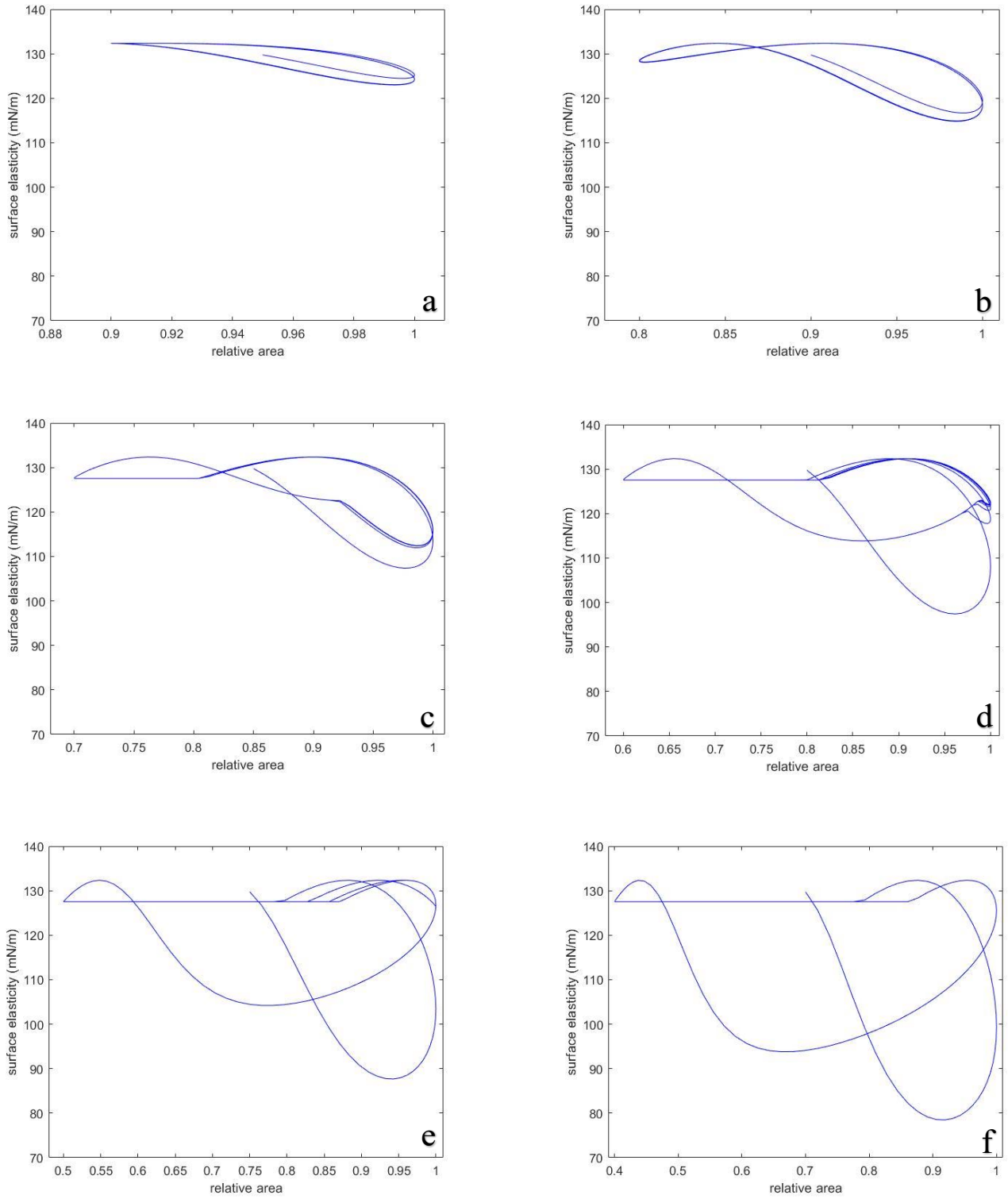

Figure 5.22: Surface elasticity (mN/m) versus relative area at a compression ratio of a) 10%, b) 20%, c) 30%, 40%d), e) 50% and f) 60%.

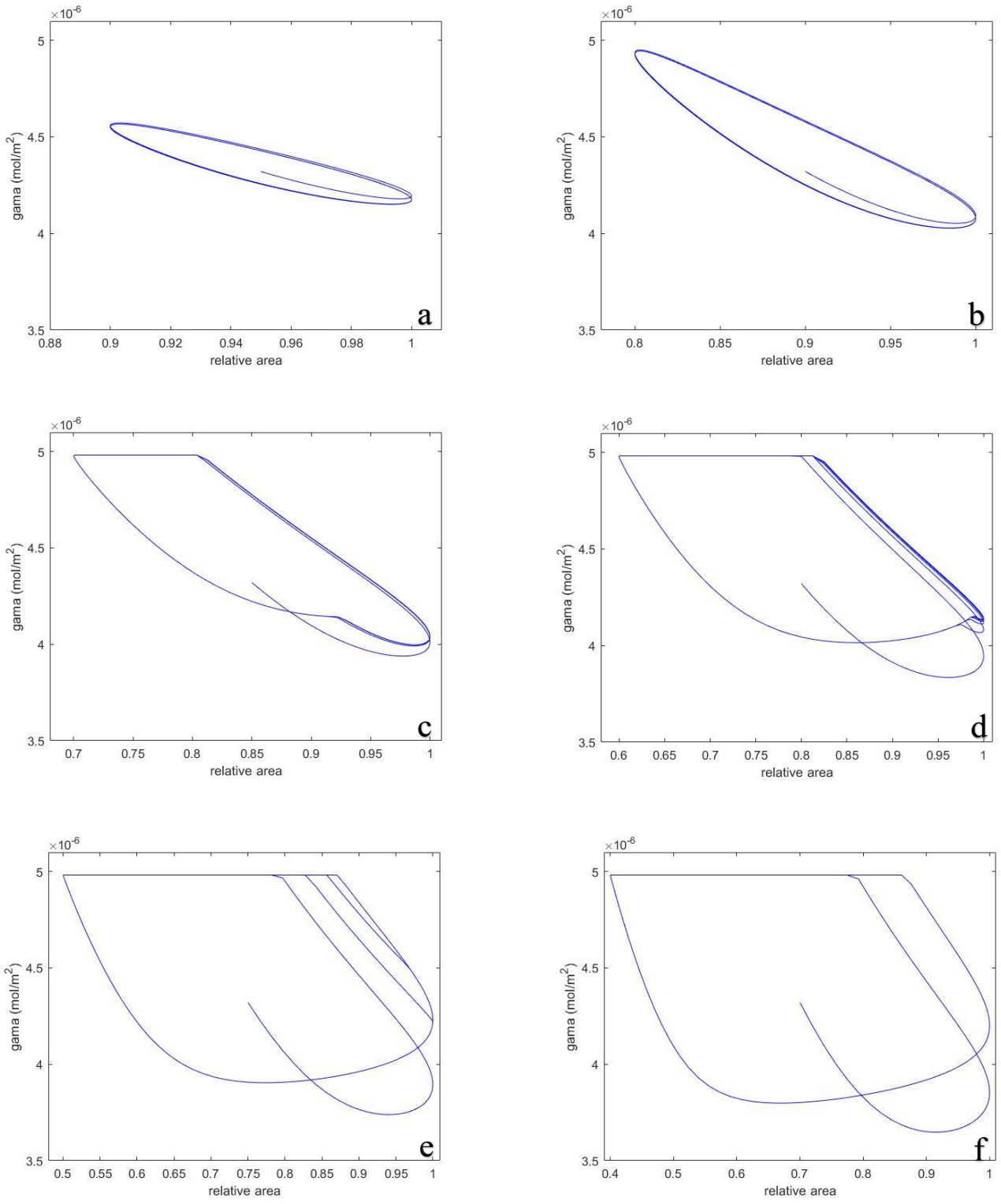

Figure 5.23: Interfacial excess (mol/m2) versus relative area at a compression ratio of a) 10%, b) 20%, c) 30%, 40%d), e) 50% and f) 60%.

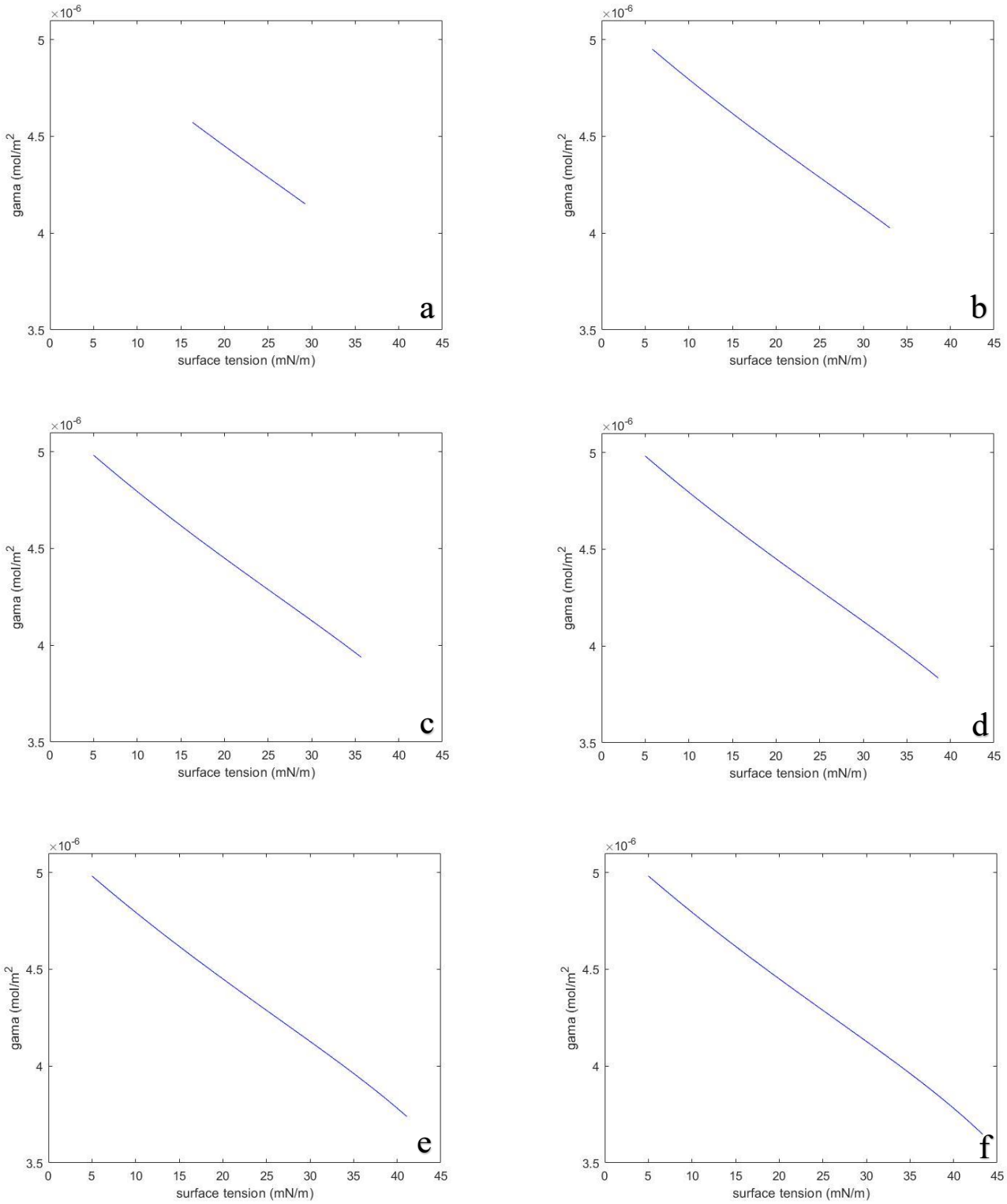

Figure 5.24: Interfacial excess (mol/m2) versus surface tension (mN/m) at a compression ratio of a) 10%, b) 20%, c) 30% ,40%d), e) 50% and f) 60%.

5.6 Runge-Kutta

The range kutta method was used in order to spot possible differences in the behavior of the surfactant due to the discretization method. For certain values of compressibility large spikes at the surface tension during expansion are observed fig. 5.13, fig. 5.21 which are not present at studies performing simulations on similar models [21], [26]. The 4th order Runge-Kutta [27] was used in order to find the solution of the initial problem proposed by eq.4.9:

$$G(t,\Gamma) = \frac{d\Gamma}{dt} = k_{ads}C_{10}[(\Gamma_{\infty} - \Gamma) - \left(\frac{\Gamma}{KC_{10}}\exp(-2a\theta)\right)] - \frac{\Gamma}{A}\frac{dA}{dt} \quad (5.1)$$

The terms $\frac{dA}{dt}$ and A are already calculated in the model. Therefore:

$$\Gamma(i+1) = \Gamma(i) + 1/6(k_1 + 2k_2 + k_3 + k_4)h \quad (5.2)$$

Where:

$$k_1 = G(\Gamma_i) \quad (5.3)$$

$$k_2 = G(\Gamma_i + 0.5k_1h) \quad (5.4)$$

$$k_3 = G(\Gamma_i + 0.5k_2h) \quad (5.5)$$

$$k_4 = h * G(\Gamma_i + k_3h) \quad (5.6)$$

$$h = \frac{t_{per}}{1000} \quad (5.7)$$

where t_{per} is the time it takes for the complete cycle of deflation and inflation of the alveoli. In this instance each cycle contains one thousand timesteps.

Chapter 6. **DISCUSSION**

The influence of the parameters according to the results shown will be discussed. The equilibrium surface tension σeq shows strong influence on the surface tension versus relative area loop fig. 5.1 as it shifts the entire loop up or down as σeq is increased or decreased respectively. It is also noted that the entire loop is widened as σeq is increased especially at the expansion part of the loop which can be also observed by the elasticity of the monolayer fig. 5.2 as the elasticity visibly lowers its value as σeq is increased.

Compressibility is the inversed elasticity [10]. As depicted in fig 5.2 by increasing the compressibility, the elasticity is notably reduced. This leads to a greater resistance in changes to the surface tension. The surface tension versus relative area loop fig 5.1 is narrowed in the cases with higher compressibility. Due to the compressibility more surfactant resides in the monolayer fig 5.3, fig 5.4.

The Frumkin parameter a as previously mentioned dictates the interactions of the adsorbed monomers. In this instance the higher the values of this parameter the stronger the attractive intermolecular forces which leads to a lower surface tension fig. 5.5 and fig 5.9. The elasticity is notably higher fig 5.6 and fig. 5.10 as the Frumkin parameter a is increased as more drastic changes in surface tension are introduced.

The kr parameter dictates the re-insertion of the surfactant from the reservoir to the adsorbed monolayer. The higher its value, the faster the re-insertion is completed and lower surface tension values are held as the alveoli expands until the reservoir is emptied fig 5.13. Since k_r influences only the rate of surfactant re-insertion from the reservoir, the amount of surfactant in the reservoir do not change.

The surface elasticity is decreased (therefore the changes in surface tension are) with increasing temperatures fig. 5.18 which is expected according to research [10], [28], [29]. The collapse of the monolayer is temperature dependent [10]. Therefore, the surface pressure at which the collapse phenomenon takes place is not necessarily the same as in the current case.

The compression ratio dictates the level of compression of the alveoli compared to its inflated state. In this case it controls the surface area of the alveoli A. When the compression

ratio is small, the reservoir is empty at the entire process since the surface pressure to reach collapse is not reached fig. 5.21. At very high compressions, the reservoir always contains surfactant ready to replenish the monolayer since there is not enough time for all the surfactant to re-insert fig. 5.21. This also explains the notably higher surface tension achieved at the inflated state of the alveoli in the cases with higher compression ratio.

The results of the Runge-Kutta method show no difference in the behavior of the surfactan between the methods of discretization and the spikes observed are attributed to the level of compression that makes the influence of the reservoir notable as well as the k_r parameter which influences the rate of transfer of surfactant from the reservoir to the monolayer.

REFERENCES

[1] Zasadzinski, J.A, et al. “The Physics and Physiology of Lung Surfactants.” Current Opinion in Colloid & Interface Science, vol. 6, no. 5-6, Nov. 2001, pp. 506–513, 10.1016/s1359-0294(01)00124-8. Accessed 10 Oct. 2021.

[2] Pérez-Gil, Jesús. “Structure of Pulmonary Surfactant Membranes and Films: The Role of Proteins and Lipid–Protein Interactions.” *Biochimica et Biophysica Acta (BBA) - Biomembranes*, vol. 1778, no. 7-8, July 2008, pp. 1676–1695, 10.1016/j.bbamem.2008.05.003. Accessed 29 Mar. 2020.

[3] Hofmann, Werner. “Modelling Inhaled Particle Deposition in the Human Lung—a Review.” Journal of Aerosol Science, vol. 42, no. 10, 1 Oct. 2011, pp. 693–724, www.sciencedirect.com/science/article/pii/S0021850211000875, 10.1016/j.jaerosci.2011.05.007. Accessed 31 Mar. 2021.

[4] Ochs, Matthias, et al. “The Number of Alveoli in the Human Lung.” *American Journal of Respiratory and Critical Care Medicine*, vol. 169, no. 1, Jan. 2004, pp. 120–124, 10.1164/rccm.200308-1107oc.

[5] Roussos, Charis, and M Campbell. “Respiratory Muscle Energetics.” Comprehensive Physiology, 1 Dec. 1986, pp. 481–509, https://doi.org/10.1002/cphy.cp030328.

[6] Grotberg, James B. “Respiratory Fluid Mechanics.” *Physics of Fluids*, vol. 23, no. 2, Feb. 2011, p. 021301, 10.1063/1.3517737. Accessed 7 Dec. 2020.

[7] Steinhart, Martin. “Physics and Chemistry of Interfaces. Von Hans-Jürgen Butt, Karlheinz Graf Und Michael Kappl.” *Angewandte Chemie*, vol. 116, no. 27, 5 July 2004, pp. 3593–3593, 10.1002/ange.200385136.

[8] Manikantan, Harishankar, and Todd M. Squires. “Surfactant Dynamics: Hidden Variables Controlling Fluid Flows.” *Journal of Fluid Mechanics*, vol. 892, 6 Apr. 2020, www.cambridge.org/core/services/aop-cambridge-core/content/view/7303EA9FF056B9B0D1EE12EE4D6D3A53/S0022112020001706a.pdf/div-class-title-surfactant-dynamics-hidden-variables-controlling-fluid-flows-div.pdf, 10.1017/jfm.2020.170. Accessed 11 Mar. 2021.

[9] “The Role of Lipids in Pulmonary Surfactant.” *Biochimica et Biophysica Acta (BBA) - Molecular Basis of Disease*, vol. 1408, no. 2-3, 19 Nov. 1998, pp. 90–108, www.sciencedirect.com/science/article/pii/S0925443998000611,10.1016/S0925-4439(98)00061-1.

[10] Wüstneck, R., et al. “Interfacial Properties of Pulmonary Surfactant Layers.” *Advances in Colloid and Interface Science*, vol. 117, no. 1, 14 Dec. 2005, pp. 33–58, www.sciencedirect.com/science/article/abs/pii/S0001868605000801, 10.1016/j.cis.2005.05.001. Accessed 22 Nov. 2021.

[11] Pérez-Gil, J., and K. M. Keough. “Interfacial Properties of Surfactant Proteins.” Biochimica et Biophysica Acta, vol. 1408, no. 2-3, 19 Nov. 1998, pp. 203–217,

pubmed.ncbi.nlm.nih.gov/9813327/, 10.1016/s0925-4439(98)00068-4. Accessed 23 Nov. 2021.

[12] Rugonyi, Sandra, et al. "The Biophysical Function of Pulmonary Surfactant." Respiratory Physiology & Neurobiology, vol. 163, no. 1-3, Nov. 2008, pp. 244–255, 10.1016/j.resp.2008.05.018. Accessed 29 Dec. 2021.

[13] Venkitaraman, A. R., et al. "Enhancement of Biophysical Activity of Lung Surfactant Extracts and Phospholipid-Apoprotein Mixtures by Surfactant Protein A." *Chemistry and Physics of Lipids*, vol. 56, no. 2-3, 1 Dec. 1990, pp. 185–194, pubmed.ncbi.nlm.nih.gov/2095991/, 10.1016/0009-3084(90)90101-v.

[14] Lee, Ka Yee C. "Collapse Mechanisms of Langmuir Monolayers." Annual Review of Physical Chemistry,vol.59,no.1,May2008,pp.771–791, leelab.uchicago.edu/papers/Annu.%20Rev.%20Phys.%20Chem.%2059%20(2008).pdf, 10.1146/annurev.physchem.58.032806.104619. Accessed 6 July 2020.

[15] Park, J. Y., and R. C. Advincula. "2 - Nanostructured Thin Films from Amphiphilic Molecules." *ScienceDirect*, Woodhead Publishing, 1 Jan. 2011, www.sciencedirect.com/science/article/pii/B9781845698126500026. Accessed 11 Mar. 2021.

[16] Zuo, Y., et al. "Current Perspectives in Pulmonary Surfactant--Inhibition, Enhancement and Evaluation." Biochimica et Biophysica Acta, 2008, www.semanticscholar.org/paper/Current-perspectives-in-pulmonary-enhancement-and-Zuo-Veldhuizen/5c507ddaf260f9796d85ef7f26aa086d1c3f0351, 10.1016/j.bbamem.2008.03.021. Accessed 31 Mar. 2022.

[17] Borwankar, R. P., and D. T. Wasan. "Equilibrium and Dynamics of Adsorption of Surfactants at Fluid-Fluid Interfaces." Chemical Engineering Science, vol. 43, no. 6, 1 Jan. 1988, pp. 1323–1337, www.sciencedirect.com/science/article/pii/0009250988851066, 10.1016/0009-2509(88)85106-6. Accessed 27 Feb. 2022.

[18] Eastoe, J, and J.S Dalton. "Dynamic Surface Tension and Adsorption Mechanisms of Surfactants at the Air–Water Interface." *Advances in Colloid and Interface Science*, vol. 85, no. 2-3, Mar. 2000, pp. 103–144, 10.1016/s0001-8686(99)00017-2. Accessed 23 June 2020.

[19] Lin, Feng, et al. "Marangoni Convection-Driven Laser Fountains on Free Surfaces of Liquids." *Materials Today Physics*, vol. 21, 1 Nov. 2021, p. 100558, www.sciencedirect.com/science/article/pii/S2542529321002194, https://doi.org/10.1016/j.mtphys.2021.100558. Accessed 8 Mar. 2022.

[20] Lunkenheimer, K., et al. "Dynamic Surface Tension and Surface Area Elasticity of Adsorbed Pulmonary Surfactant Layers." *Colloids and Surfaces A: Physicochemical and Engineering Aspects*, vol. 114, 20 Aug. 1996, pp. 199–210, www.sciencedirect.com/science/article/pii/0927775796036928, 10.1016/0927-7757(96)03692-8. Accessed 12 Oct. 2022.

[21] Bouchoris, K., and V. Bontozoglou. "A Model of Lung Surfactant Dynamics Based on Intrinsic Interfacial Compressibility." *Colloids and Surfaces A: Physicochemical and Engineering Aspects*, vol. 624, 5 Sept. 2021, p. 126839, www.sciencedirect.com/science/article/pii/S0927775721007081, 10.1016/j.colsurfa.2021.126839. Accessed 5 June 2022.

[22] Kovalchuk, V.I., et al. “Dilational Rheology of Adsorbed Surfactant Layers—Role of the Intrinsic Two-Dimensional Compressibility.” *Advances in Colloid and Interface Science*, vol. 114-115, June 2005, pp. 303–312, 10.1016/j.cis.2004.08.007. Accessed 28 Mar. 2022.

[23] Kovalchuk, V. I., G. Loglio, V. B. Fainerman, and R. Miller. 2004. “Interpretation of Surface Dilational Elasticity Data Based on an Intrinsic Two-Dimensional Interfacial Compressibility Model.” *Journal of Colloid and Interface Science* 270 (2): 475–82. https://doi.org/10.1016/j.jcis.2003.07.017.

[24] Fisher, Martin J., et al. “Determination of Alveolar Surface Area and Tension from in Situ Pressure-Volume Data.” Respiration Physiology, vol. 10, no. 2, Sept. 1970, pp. 159–171, 10.1016/0034-5687(70)90080-0. Accessed 22 Aug. 2019.

[25] Chang, Chien-Hsiang, and Elias I. Franses. “Adsorption Dynamics of Surfactants at the Air/Water Interface: A Critical Review of Mathematical Models, Data, and Mechanisms.” Colloids and Surfaces A: Physicochemical and Engineering Aspects, vol. 100, no. 100, 25 July 1995, pp. 1–45, www.sciencedirect.com/science/article/abs/pii/0927775794030614, 10.1016/0927-7757(94)03061-4.

[26] Morris, J., et al. “Dynamic Behavior of Lung Surfactant.” *Journal of Biomechanical Engineering*, vol. 123, no. 1, 1 Feb. 2001, pp. 106–113, pubmed.ncbi.nlm.nih.gov/11277295/, https://doi.org/10.1115/1.1336146. Accessed 27 Feb. 2024.

[27] Rojas, L, et al. “Modeling of Dynamic Mass Coupled System with Runge-Kutta Fourth Order.” *IOP Conference Series: Materials Science and Engineering*, vol. 519, no. 1, 1 May 2019, p. 012009, https://doi.org/10.1088/1757-899x/519/1/012009. Accessed 25 May 2022.

[28] Cheng, Li Yaw (Michael), and Su Min (Lisa) Wei. “Investigation of Surfactant Surface Tension and Its Correlation with Temperature and Concentration.” Open.library.ubc.ca, 2012, open.library.ubc.ca/soa/cIRcle/collections/undergraduateresearch/51869/items/1.0107233.

[29] Bykov, A.G., et al. “Influence of Temperature on Dynamic Surface Properties of Spread DPPC Monolayers in a Broad Range of Surface Pressures.” *Chemistry and Physics of Lipids*, vol. 225, Dec. 2019, p. 104812, https://doi.org/10.1016/j.chemphyslip.2019.104812.